

AD-A032 007

EG AND G INC ALBUQUERQUE N MEX
FIVE-CHANNEL MICROWAVE SYSTEM. (U)

AUG 76 D L TRONE, G D SOWER

UNCLASSIFIED

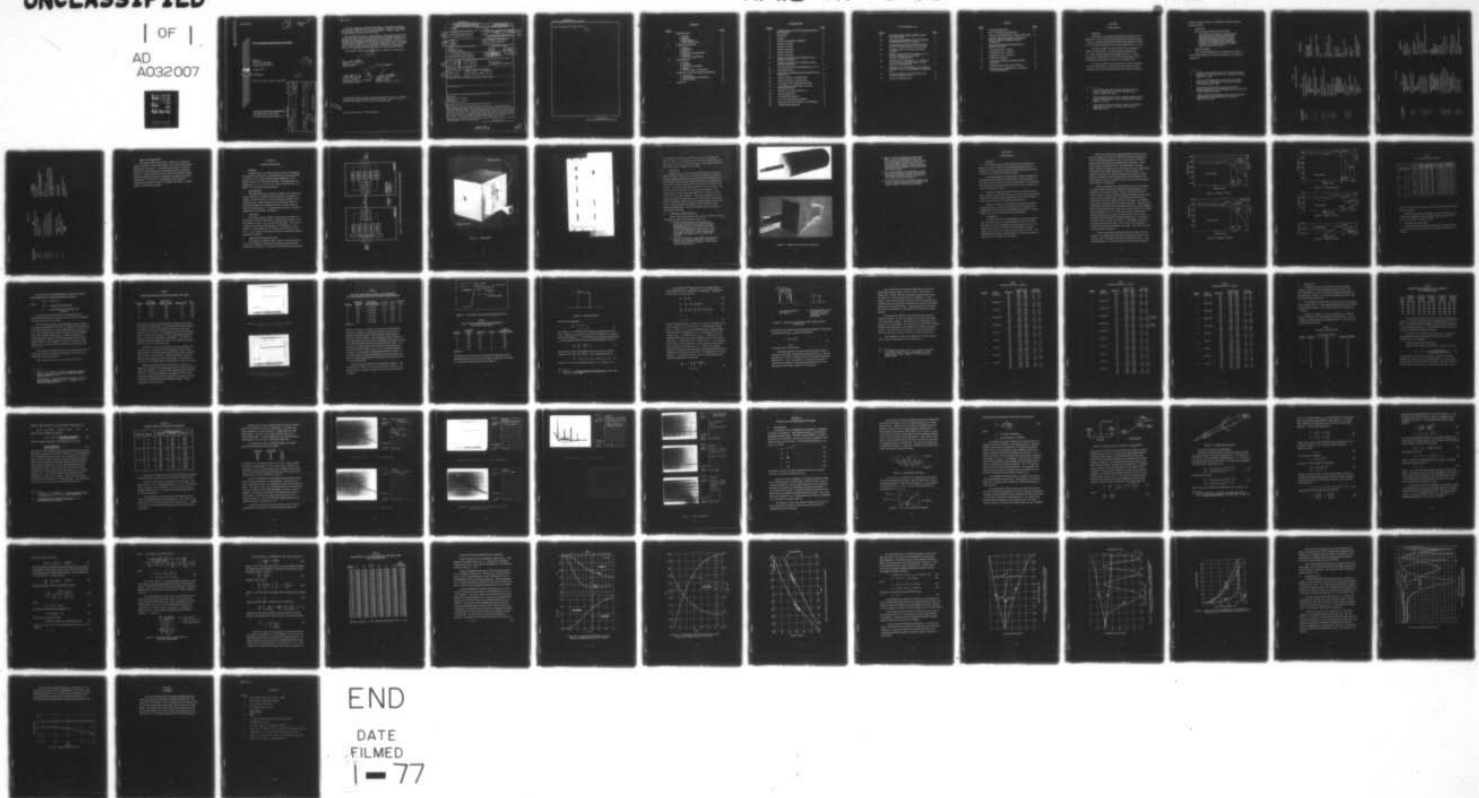
| OF |
AD
A032007

AFWL-TR-76-71

F/G 17/2.1

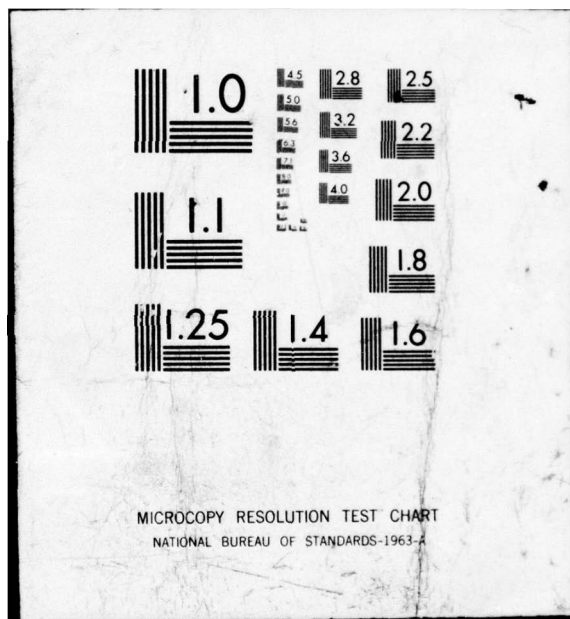
F29601-75-C-0131

NL



END

DATE
FILMED
1-77



AD A 032 007

AFWL-TR-76-71

AFWL-TR-
76-71



FIVE-CHANNEL MICROWAVE SYSTEM

EG&G Inc.
9733 Coors Road NW
Albuquerque, NM 87114

August 1976

Final Report

Approved for public release; distribution

RECORDED
RECORDED
RECORDED
RECORDED
RECORDED

AD NUMBER AD. A032 007		<input type="checkbox"/> CHECK IF THIS IS A NEW SOURCE.
CATALOGER vb		
DDC	FORM 149 JAN 69	DATE 17 Nov 76
AIR FORCE WEAPONS LABORATORY Air Force Systems Command Kirtland Air Force Base, NM 87117 NEW CONTRACT		

CODE NO.
388 316

CONTRACT
F29601-75-C-0131

GRANT

SOURCE
EG and G Inc. Albuquerque, N. Mex.

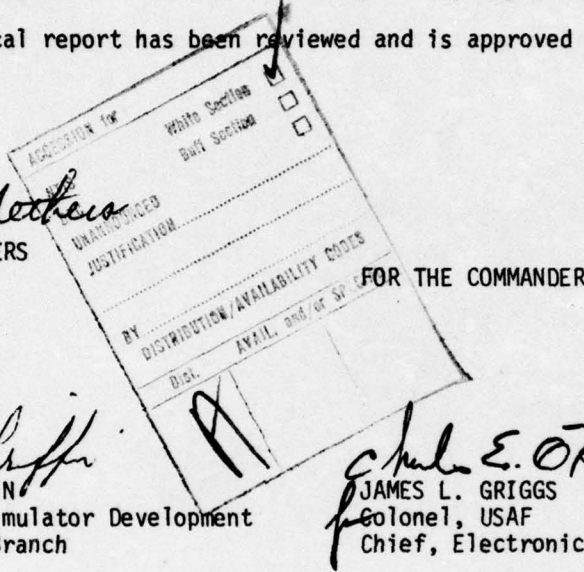
This final report was prepared by the EG&G Inc., Albuquerque, New Mexico, under Contract F29601-75-C-0131, Job Order 12090306, with the Air Force Weapons Laboratory, Kirtland Air Force Base, New Mexico. Raymond W. Nethers (ELS) was the Laboratory Project Officer-in-Charge.

When US Government drawings, specifications, or other data are used for any purpose other than a definitely related Government procurement operation, the Government thereby incurs no responsibility nor any obligation whatsoever, and the fact that the Government may have formulated, furnished, or in any way supplied the said drawings, specifications, or other data is not to be regarded by implication or otherwise as in any manner licensing the holder or any other person or corporation or conveying any rights or permission to manufacture, use, or sell any patented invention that may in any way be related thereto.

This technical report has been reviewed and is approved for publication.

Raymond W. Nethers

RAYMOND W. NETHERS
Project Officer



Albert B. Griffin
ALBERT B. GRIFFIN
Acting Chief, Simulator Development
and Operations Branch

James L. Griggs
JAMES L. GRIGGS
Colonel, USAF
Chief, Electronics Division

This report has been reviewed by the Information Office (OI) and is releasable to the National Technical Information Service (NTIS). At NTIS, it will be available to the general public, including foreign nations.

DO NOT RETURN THIS COPY. RETAIN OR DESTROY.

UNCLASSIFIED

SECURITY CLASSIFICATION OF THIS PAGE (When Data Entered)

REPORT DOCUMENTATION PAGE			READ INSTRUCTIONS BEFORE COMPLETING FORM
1. REPORT NUMBER AFWL-TR-76-71	2. GOVT ACCESSION NO.	3. RECIPIENT'S CATALOG NUMBER	
(6) FIVE CHANNEL MICROWAVE SYSTEM		(9) 4. TYPE OF REPORT & PERIOD COVERED Final Report Jun 75-Feb 76	
(10) D. L. Trone G. D. Sower		5. PERFORMING ORG. REPORT NUMBER	
9. PERFORMING ORGANIZATION NAME AND ADDRESS EG&G Inc. 9733 Coors Rd. NW Albuquerque, NM 87114		10. PROGRAM ELEMENT, PROJECT, TASK AREA & WORK UNIT NUMBERS 64747F 12090306	
11. CONTROLLING OFFICE NAME AND ADDRESS Air Force Weapons Laboratory (ELS) Kirtland Air Force Base, NM 87117		12. REPORT DATE August 1976	
14. MONITORING AGENCY NAME & ADDRESS (if different from Controlling Office) (16) 1209 (17) 03		15. SECURITY CLASS. (of this report) Unclassified	
16. DISTRIBUTION STATEMENT (of this Report) Approved for public release; distribution unlimited.		15a. DECLASSIFICATION/DOWNGRADING SCHEDULE	
(18) AFWL (19) TR-76-71		17. DISTRIBUTION STATEMENT (of the abstract entered in Block 20, if different from Report)	
18. SUPPLEMENTARY NOTES			
19. KEY WORDS (Continue on reverse side if necessary and identify by block number) Microwave Data Transmission Systems Telemetry EMP Measurement Systems			
20. ABSTRACT (Continue on reverse side if necessary and identify by block number) This document describes the development and production of 5-channel microwave data transmission systems. These systems are to provide a 300 foot data link to transmit measurement data from a test object such as a missile or aircraft placed in an EMP test facility to a shielded instrumentation room or trailer where the data can be recorded. The systems can be used in any test facility that requires up to 300 feet isolation between the test object and the instrumentation recording system. These systems were designed and fabricated under (over)			

DD FORM 1 JAN 73 1473 EDITION OF 1 NOV 65 IS OBSOLETE

UNCLASSIFIED
SECURITY CLASSIFICATION OF THIS PAGE (When Data Entered)

388316

JR

UNCLASSIFIED

SECURITY CLASSIFICATION OF THIS PAGE(When Data Entered)

Air Force Contract No. F29601-75-C-0131.

1

UNCLASSIFIED

SECURITY CLASSIFICATION OF THIS PAGE(When Data Entered)

CONTENTS

<u>Section</u>		<u>Page</u>
I	INTRODUCTION	5
	1 General	5
	2 Objective	6
	3 Specifications	6
	4 Report Organization	10
II	SYSTEM DESCRIPTION	11
	1 General	11
	2 Transmitter	11
	3 Receiver	11
	4 Dielectric Waveguide (DWG)	11
	5 Operation	15
	6 Significant Improvements	15
III	TEST RESULTS	18
	1 General	18
	2 Bandwidth	18
	3 Risetime and Overshoot	22
	4 Stability	35
	5 Dynamic Range and Distortion	36
IV	EFFECTS OF THE DIELECTRIC WAVEGUIDE	44
	1 Background	44
	2 DWG Attenuation and Dispersion	48
	3 Empirical Data	63
V	SUMMARY	66

ILLUSTRATIONS

<u>Figure</u>		<u>Page</u>
1	5 Channel Microwave Data Transmission System Block Diagram	12
2	Transmitter	13
3	Receiver	14
4	Dielectric Waveguide Components	16
5	Channel 1 CW Data	20
6	Channel 2 CW Data	20
7	Channel 3 CW Data	21
8	Channel 4 CW Data	21
9	Channel 5 CW Data	21
10	Response of Typical DLT-7 Channel to 70 ps. Risetime Input Pulse	25
11	Response of Typical DLT-7 Channel to Slower Risetime Input Pulse	25
12	Characteristic Step-Function Response of DLT-7	27
13	Input Step Function	28
14	Illustration of Successive Fourier Approximations (Reference 9)	30
15	Channel 1/System 1 Linearity Data	40
16	Channel 4/System 2 Linearity Data	40
17	Transmitter Video Amplifier Input Ramp	41
18	Ramp Output for System with 3.9 Percent Harmonic Distortion	41
19	Harmonics of System of Figure 18	42
20	Dynamic Range Data	43
21	AM Modulation Envelope	45
22	k vs ω for Conventional Waveguide	45
23	Spectrum and Vector Diagram of AM Modulation	47
24	Envelope Delay Distortion	48

ILLUSTRATIONS (cont)

<u>Figure</u>		<u>Page</u>
25	Attenuation Factor versus Diameter in Free-Space Wavelengths	52
26	Velocities and Wavelength in 5/8-inch Diameter Polyethylene Rod (4.0 to 17.0 GHz)	56
27	Group Velocity and Arrival Time for 5/8-inch Diameter Polyethylene Rod (8.5 to 12.0 GHz)	57
28	Attenuation and Arrival Time for 5/8-inch Diameter	58
29	Relative Arrival Times for Sidebands ($f_0 = 11.0$ GHz) for 100-Meter Long, 5/8-inch Diameter Polyethylene Rod	60
30	Relative Power Transmitted ($f_0 \approx 11.0$ GHz) for each Sideband for 100-Meter Long, 5/8-inch Diameter Polyethylene Rod	61
31	Phase Error in Each Sideband ($f_0 = 11.0$ GHz) for 100-Meter Long, 5/8-inch Diameter Polyethylene Rod	62
32	Empirical Relative Power Data for 5/8-inch Diameter Polyethylene Rod	64
33	Empirical Attenuation Data	65

TABLES

<u>Table</u>		<u>Page</u>
1	Contract Specifications	7
2	DLT-7 Bandwidth Characteristics	22
3	Risetime/Bandwidth Data for System 3 (300' DWG)	24
4	Risetime, Bandwidth, Ripple, and Overshoot Data for System 2 (System 3) in Bench Configuration	26
5	Step-Function Response Characteristics of System 2 (System 3)	27
6	Temperature Test - System 1	32
7	Temperature Test - System 2	33
8	Temperature Test - System 3	34
9	Stability Test Results	35
10	Temperature Stability of Calibration Pulse Generators	36
11	Dynamic Range and Harmonic Distortion	38
12	Properties of 5/8-inch Diameter, 100-Meter Long Polyethylene Rod	54

SECTION I

INTRODUCTION

1 GENERAL

This report is a summary of EG&G's efforts under contract F29601-75-C-0131. More detailed information concerning the three 5-channel microwave Dielectric Waveguide (DWG) systems developed for AFWL under this contract can be found in References 1, 2, and 3.

The Project Officer for this contract was Mr. Raymond W. Nethers of AFWL/ELSE. The EG&G Program Manager was J. C. Giles, and the EG&G Project Engineer was D. L. Trone. The period of performance was June 1975 through February 1976; the hardware was delivered to AFWL on 15 December 1975.

The three systems developed under this contract, designated by EG&G as Model DLT-7, represent a further improvement and evolution of the X-band EMP data telemetry links built by EG&G for

1. "Five-Channel Microwave System Acceptance Test Procedures," EG&G Report AL-1183, 29 August 1975, Contract F29601-75-C-0131.
2. "Five-Channel Microwave System Operation and Maintenance Manual," EG&G Report AL-1199, 6 January 1976, Contract F29601-75-C-0131.
3. "Five-Channel Microwave System Acceptance Test Report," EG&G Report AL-1208, 27 February 1976, Contract F29601-75-C-0131.

AFWL and others since 1969. References 4 through 7 describe previous systems.

2 OBJECTIVE

Per the contract Statement of Work (SOW),

"The objective of this effort is to develop and fabricate three five-channel microwave data transmission systems to operate in a high intensity electromagnetic environment and to transmit wide bandwidth data via dielectric waveguide to a shielded location up to 300 feet distance from the transmitter."

3 SPECIFICATIONS

The contract specifications are summarized in Table 1. A more detailed explanation of these specifications can be found in Reference 3.

- 4. "ALECS G Single-Channel Microwave Telemetry System — Final Report," EG&G Report AL-319, June 1969, Contract F29601-69-C-0033.
- 5. "ALECS G Ten-Channel Microwave Telemetry System — Final Report," EG&G Report AL-360, December 1969, Contract F29601-69-C-0033.
- 6. "ARES Dielectric Waveguide System Operation and Maintenance Instructions," EG&G Report AL-438, June 1970, Contract F29601-69-C-0004.
- 7. "Single-Channel Wideband Microwave Telemetry Systems," EG&G Report AL-638, September 1971, Contract DAHC-60-71-C-0064.

Table 1
CONTRACT SPECIFICATIONS

SOW Paragraph	Item	Specification
4.1.1.1	Channel Capacity per System	5
4.1.1.2	Individual Data Channel Bandpass	
	Lower End	±1 dB at 10 kHz
	Upper End (required)	-3 dB at 100 MHz
	Upper End (design goal)	-1 dB at 130 MHz
	Ripple	±1 dB from 15 kHz to 80 MHz
4.1.1.3	Individual Channel Stability at Constant Temperature over 4 hours	
	Gain	±0.5 dB from 10 kHz to 100 MHz
	Phase	±3° at 100 MHz
4.1.1.4	Isolation between Channels	60 dB
4.1.1.5	Dynamic Range with all Harmonics Down by 46 dB	46 dB
4.1.1.6	Carrier Frequency	X-Band (8 to 12 GHz)
4.1.1.7	Modulation Type	Optional (double side band AM)
4.1.1.8	Overall System Video Gain	26 dB
4.1.1.9	Calibration Pulse	
	Amplitude after 100 ns	±10 mV (± 1%)
	Width (positive pulse)	200 ± 10 ns
	Width (negative pulse)	2000 ± 100 ns
	Risetime (10-90%)	10 ns
	Overshoot	10%
4.1.1.10	Pneumatic Controls	Operate/CAL - ON/OFF
4.1.1.11	DWG Length	0 to 300 feet
4.1.2.1	Transmitter Input Impedances	
	Unbalanced	50 ohms (± 2%)
	Balanced	100 ohms
Balun Transfer Function		
Ripple		±2 dB from 10 kHz to 130 MHz
ET Product		80 volt microseconds
CMR		36 dB at 110 MHz

Table 1 (cont.)

SOW Paragraph	Item	Specification
4.1.2.2	Transmitter Input Connectors	OSM, 3mm GR874 (TCC-2A) 4-inch diameter
	Unbalanced (50 ohms)	
	Balanced (100 ohms)	
	Flange	Internal
4.1.2.3	Transmitter Calibration Switch	
4.1.2.4	Transmitter Input Attenuator	0 to 80 dB or more 3 dB or smaller ± 1%
	Range	1.0 W continuous, 1000 W peak
	Steps	10 mV to 160 V pp
	Accuracy	Attenuator only
	Power Dissipation	± 2.5% of Cal pulse amplitude in 100 kV/m field
4.1.2.5	Transmitter Input Range	
4.1.2.6	Transmitter Adjustments	
4.1.2.7	Transmitter Shielding	
4.1.2.8	Transmitter Power Supply	5 hours 6 hours 16 hours or less Cal pulse clip 3 required
	Battery Life (required)	
	Battery Life (design goal)	
	Charging Cycle	
	Low Voltage Indicator	
	Battery Charger	
	Receiver Output Connector	50 ohms BNC
	Receiver Signal Strength Indicator	Each Channel
	Receiver Pneumatic Control System	ON/OFF - OPERATE /CAL
	Receiver Power Requirements	95 - 130 VAC, 60 ± 3 Hz
	Receiver Trigger Signal	
	Output Connector	50 ohms BNC
	Amplitude with Cal Pulse	0.5 V, Electrically Isolated
	Transmitter Case Size	1.5 ft x 2 ft x 2 ft or less
4.2.1.1	Transmitter Weight	100 lbs or less
4.2.1.2	Transmitter Finish	Electrically Conductive and Corrosion Resistant
4.2.1.3		

Table 1 (cont.)

<u>SOW Paragraph</u>	<u>Item</u>	<u>Specification</u>
4.2.1.4	Transmitter Controls and Connector	Easily Accessible
4.2.1.5	Transmitter Case Opening	Easily Opened
4.2.2.1	Receiver Size	19-inch rack chassis with height 6 ft or less for each 5-channel system
4.2.2.2	Air Line Connections	On rear
4.2.2.3	Receiver Front Panel Finish	Dark Grey Enamel
4.3.1.1	Transmitter and Receiver Shock	30 g, 1/2 sine, 11 ms, 2 shocks per axis
4.3.1.2	Transmitter and Receiver Vibration	0.025-inch pp displacement 4 g at 55 Hz; 10 Hz to 55 Hz to 10 Hz cycle in 1 min for 15 cycles
4.3.1.3	Temperature Specification	+30° F to +120° F
	Range	+1 dB for 30° F
	Transfer Function Change	
4.3.2	Dielectric Waveguide	10 at 10 feet - 60 at 20 feet
	Lengths	0.75 inch or less
	Diameter	300 feet

4 REPORT ORGANIZATION

This report contains five sections. Section II is a brief description of the DLT-7 five-channel system; a more detailed description can be found in Reference 2. This Section also includes a brief description of the most significant accomplishments made in developing the DLT-7. Section III discusses some of the more significant results from the acceptance testing; more extensive test results can be found in Reference 3. Section IV is a presentation of theoretical and empirical results from the effects of the DWG on the signals. Finally, Section V summarizes the report.

SECTION II

SYSTEM DESCRIPTION

1 GENERAL

The Model DLT-7 microwave system is used for transmitting wide bandwidth, high dynamic range information over short distances. It consists of a five-channel EMP-hardened transmitter, a five-channel receiver and a dielectric waveguide. The operating carrier frequencies are: 9.2, 9.8, 10.4, 11.0, and 11.6 GHz (X-band). See Figure 1 for a basic system block diagram.

2 TRANSMITTER

The transmitter shown in Figure 2 contains 5 video attenuators, 5 video amplifiers, 5 calibration pulse generators, 5 modulators, 5 isolators, 5 Gunn oscillators, a five-element coaxial diplexer, and a waveguide flange. Signal connections are made through either an OSM connector panel (for unbalanced signals) or a balun connector panel (for balanced signals). The panels are removable. See system specifications in Subsection 3 of Section I.

3 RECEIVER

The receiver shown in Figure 3 (which can be operated up to 300 feet away from the transmitter) is normally rack-mounted. It can be mounted on a bench or in a screen box if necessary. The receiver contains a five-element coaxial diplexer, 5 RF attenuators, 5 RF detectors, 5 video amplifiers, and 5 meters and meter drive amplifiers. It also contains the pneumatic controls for transmitter operation (operate and calibrate).

4 DIELECTRIC WAVEGUIDE (DWG)

The Dielectric Waveguide (DWG), which is in interchangeable 10 and 20 foot lengths, provides the transmission path between the transmitter and receiver. It consists of 5/8-inch diameter polyethylene

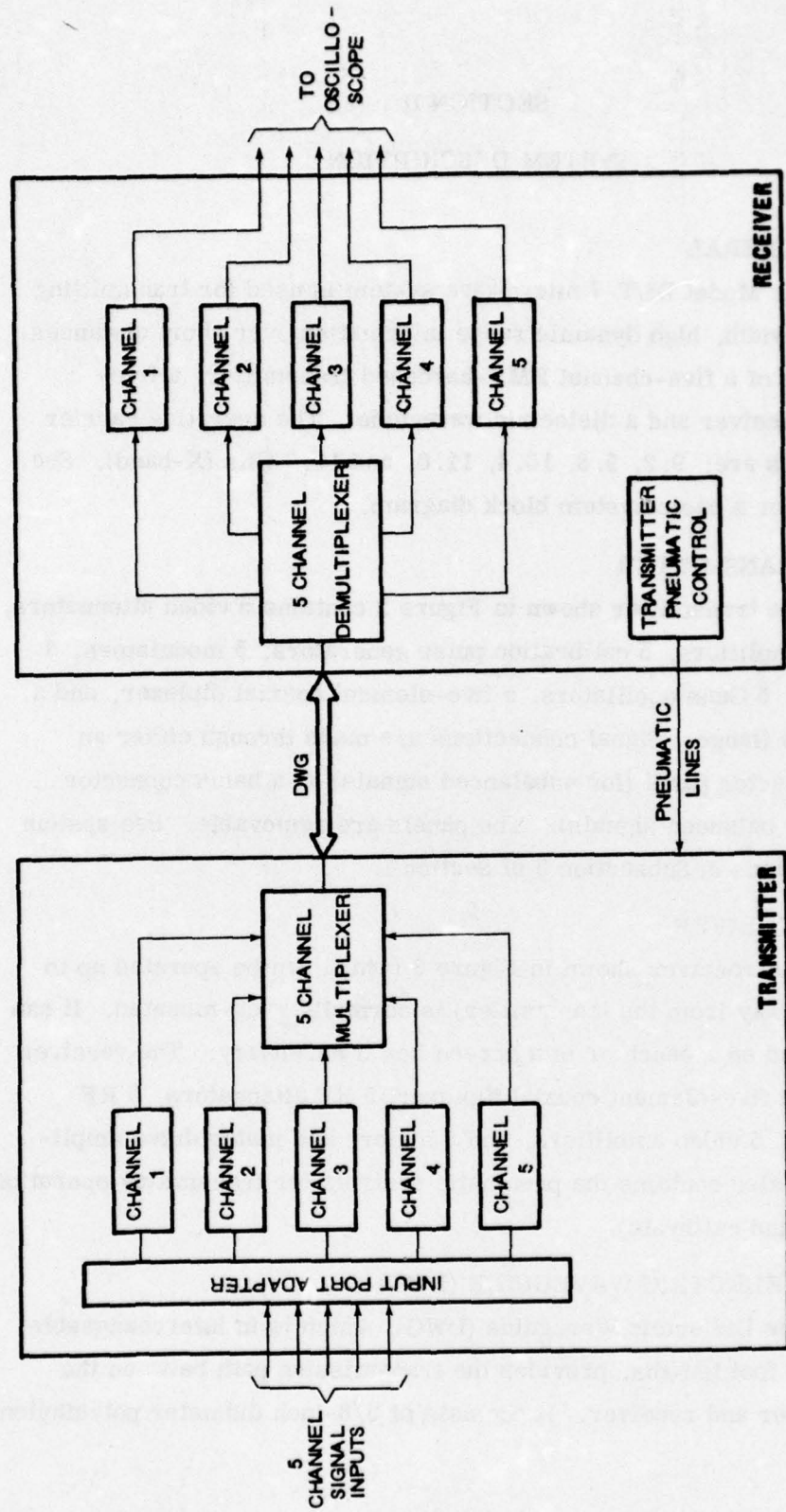


Figure 1. 5 Channel Microwave Data Transmission System Block Diagram

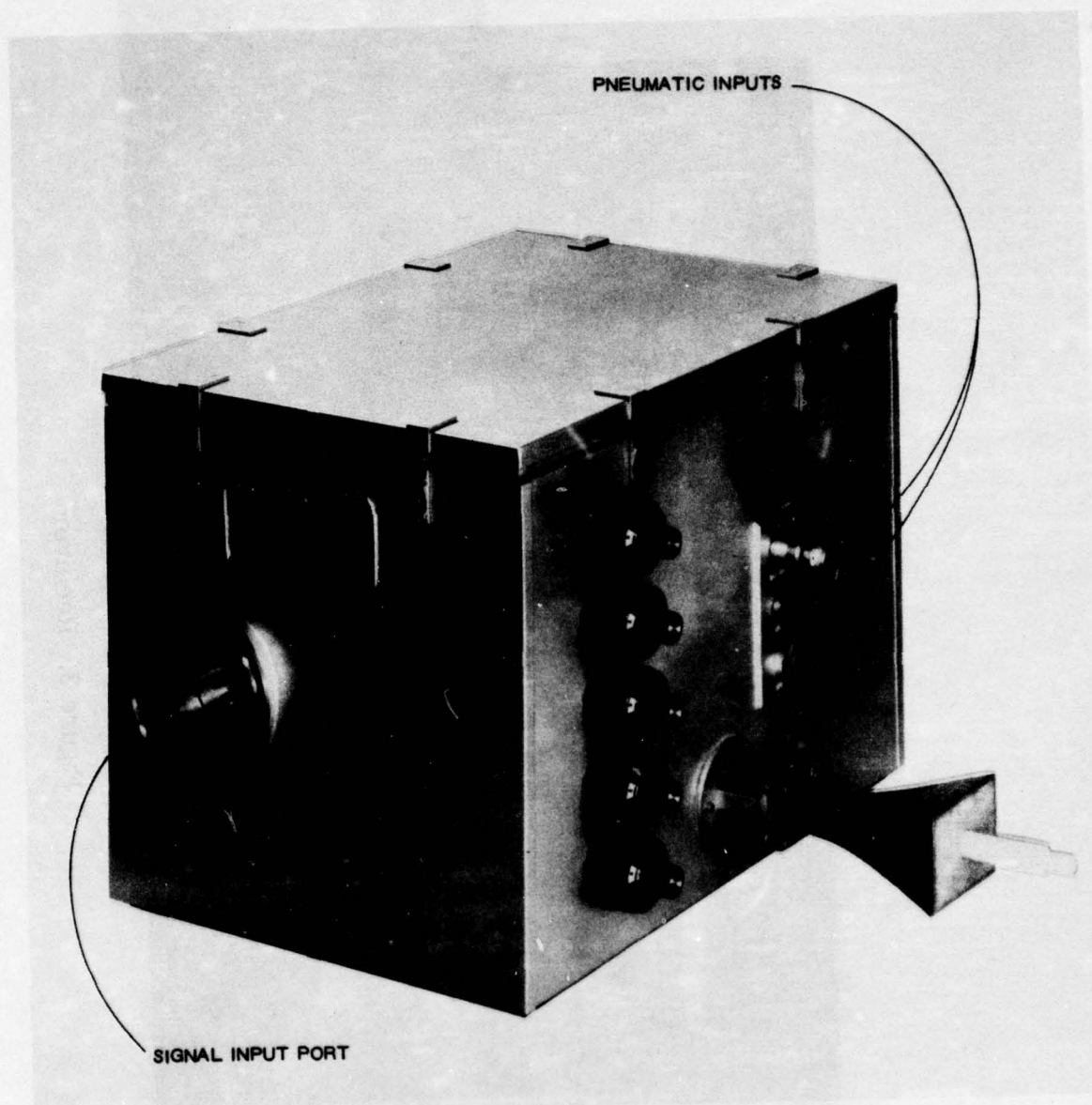


Figure 2. Transmitter

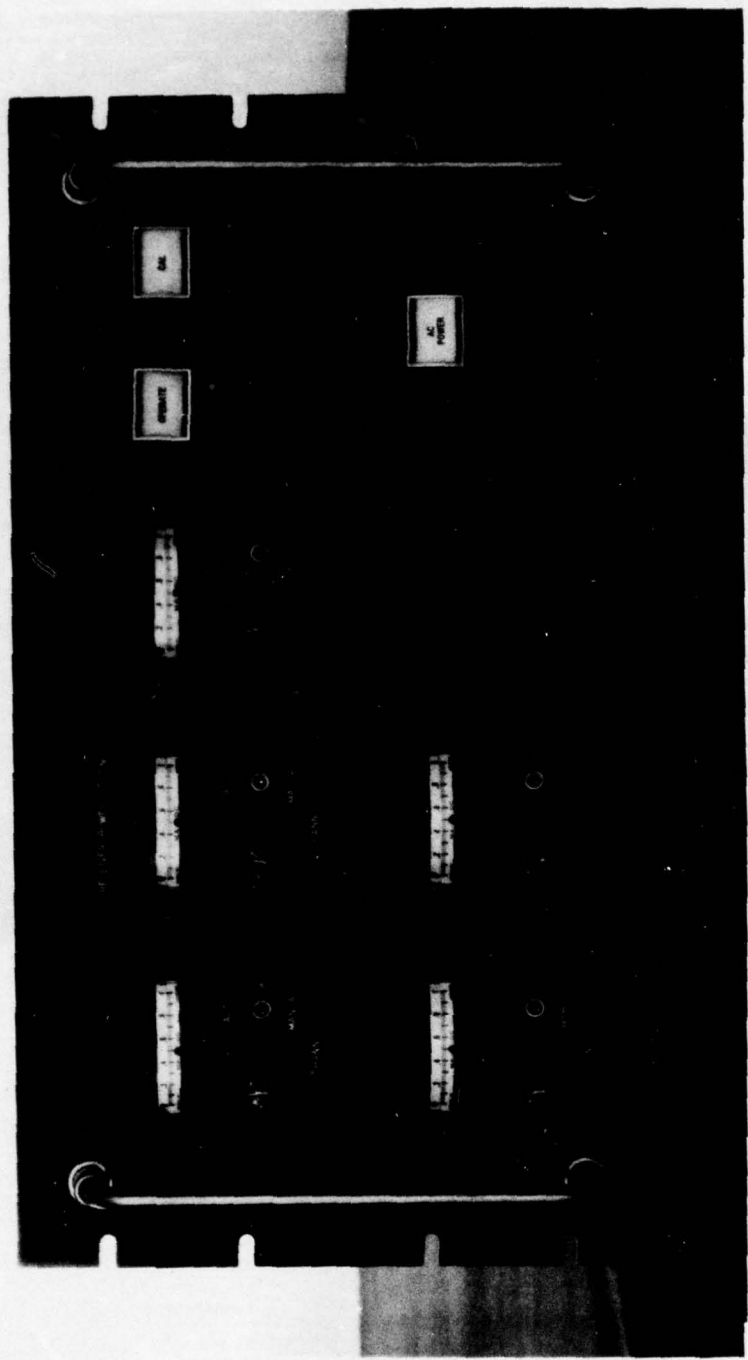


Figure 3. Receiver

rod, Ethafoam washers, and metallic-to-dielectric transitions all shown in Figure 4. The Ethafoam washers keep the polyethylene rods away from the ground or surrounding objects. For weather protection, plastic tubing can be installed over the DWG.

5 OPERATION

Signals from up to five measuring devices are fed to the transmitter by cables. There they are attenuated (if necessary) and fed to the video amplifiers and then to the modulators which amplitude modulate the Gunn-derived carriers. These AM carriers are diplexed and the composite carrier propagated down the dielectric waveguide to the receiver. Automatically adjustable attenuators in the receiver control the RF level to each detector for optimum linear operation. The crystal detectors extract the information from the carriers and send it to the receiver video amplifiers. These video amplifiers boost the signals to make them compatible with oscilloscope input requirements. Part of the detector output is coupled to a high-impedance meter driver circuit. The meter gives the operator a visual indication of the detector operating level. The video amplifier output is available on the receiver rear panel.

6 SIGNIFICANT IMPROVEMENTS

Some of the more significant improvements of the DLT-7 system over earlier single and multichannel systems are:

- The transmitter package is much smaller and easier to use than the previous ARES and ALECS multichannel systems. The package dimensions (excluding DWG transition) are 13.5 in x 13.5 in x 17.0 in, well under contract specifications. The lid is easily removable by 6 quick release latches. The double-wall design provides excellent EMP shielding.
- The receiver chassis is much smaller than previous systems and contract specifications. The chassis height is only 10 inches compared to 6 feet allowable by contract specification.

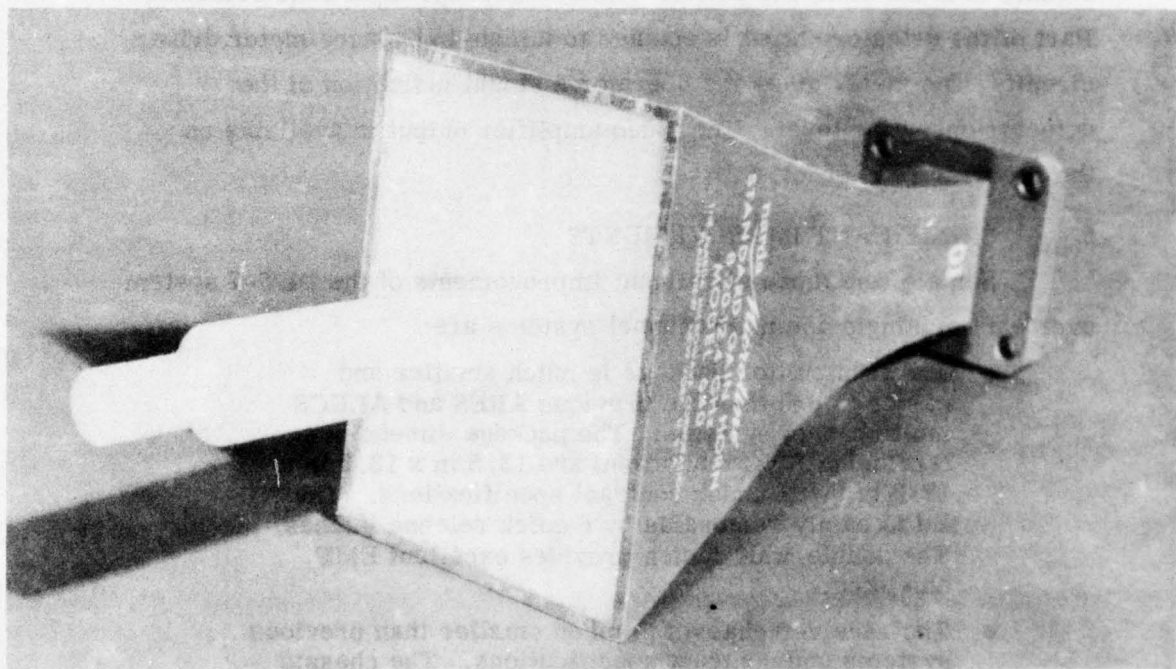
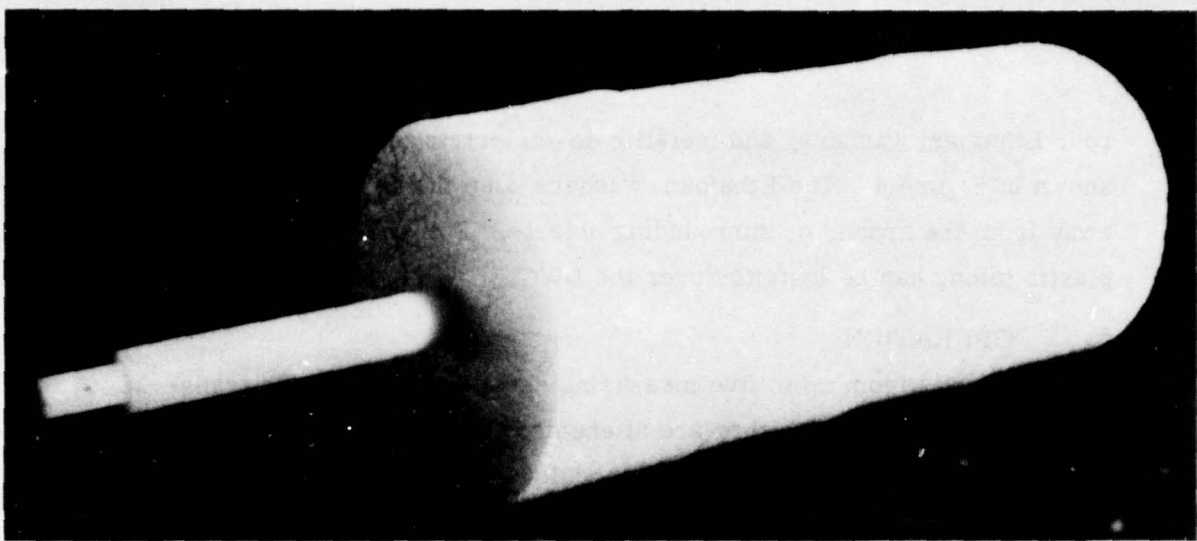


Figure 4. Dielectric Waveguide Components

- Special modulators, developed by EG&G under IR&D, are more efficient than previous ones. They permitted the elimination of costly traveling wave tube amplifiers in the receivers thereby saving money (about \$5000 per channel) and space, improving system reliability, and providing 6 dB more dynamic range.
- New coaxial diplexers were developed for EG&G. These greatly decreased package size and weight. Development problems, however, did result in a slip in delivery of the three systems.
- An automatic gain control circuit was added to each receiver channel to adjust the RF attenuation to the optimum setting to keep video gain constant.

SECTION III

TEST RESULTS

1 GENERAL

All acceptance test procedures and results are presented in References 1 and 3. Only the more significant results will be discussed here. The systems met almost all performance specifications, and those not completely met will be discussed.

It is important that the instrumentation faithfully reproduce the actual EMP-induced signals in a test program. Any perturbation by the instrumentation must be documented, reproducible, and understood. The discussions which follow address important issues related to DWG microwave telemetry systems.

During the acceptance testing of the three 5-channel systems, pulse, linearity, and bandwidth data were recorded on each data channel to correlate what effect each parameter has on the overall transfer function characteristics of the individual data channels.

Extensive testing also included phase and amplitude stability, temperature tests, and shock and vibration tests to determine the repeatability of the data links and temperature and physical movement effects on the overall transfer function characteristics.

2 BANDWIDTH

Probably the most critical specifications in this development effort are those related to system bandwidth over 300 feet of DWG. The contract requires the amplitude transfer function of every data channel to be down not more than 3 dB at 100 MHz and to have a ripple of not more than ± 1 dB over the band 15 kHz to 80 MHz. The original RFP specification and ultimately the contract design goal is to be down not more than 1 dB at 130 MHz.

EG&G did not believe the original specification could be met in all 5 data channels over 300 feet of DWG even using TWT amplifiers due to the dispersion properties of the rod at the lowest carrier frequency and the attenuation at the highest carrier frequency. Thus a 200 foot length was proposed with a -3 dB bandwidth of 130 MHz. AFWL could not accept less than a 300 foot link due to test requirements but reduced the bandwidth requirement to -3 dB at 100 MHz. By extensively testing a four-channel system then being built for another customer, EG&G found that this specification could probably be met and accepted it; however, the insertion loss of the new coaxial diplexers still remained to be quantified.

Figures 5 through 9 show the final gain curves for each channel of System 3 both in the "Bench" configuration (approximately one foot of DWG) and with 300 feet of DWG. Figure 6 also includes data for 200 feet of DWG. Because of network analyzer limitations, these curves do not go below 100 kHz; however, data was taken manually down to 10 kHz and the curve was found to be flat in this region. Note that the system gain is nominally 24 dB, not 26 dB as specified. This is because with 300 feet of DWG and with 2 dB insertion loss in each coaxial diplexer there is not sufficient carrier power at the receiver detector at the higher carrier frequencies to run at a video gain of 26 dB. Only Channel 5 meets the design goal of -1 dB at 130 MHz, but all channels meet or exceed the contract bandwidth and ripple specifications. The effects of the DWG can be seen clearly in Figure 6. As the length is increased, the upper cutoff frequency drops. Also as the carrier frequency is increased, the upper cutoff frequency increases. This will be discussed in greater detail in Section IV.

Table 2 summarizes the bandwidth characteristics of all three systems. All channels meet the contract specifications (ripple is over the band 10 kHz to 80 MHz), and 3 of the 15 channels meet the -1 dB at 130 MHz design goal. Note that System 2 has two anomalous channels

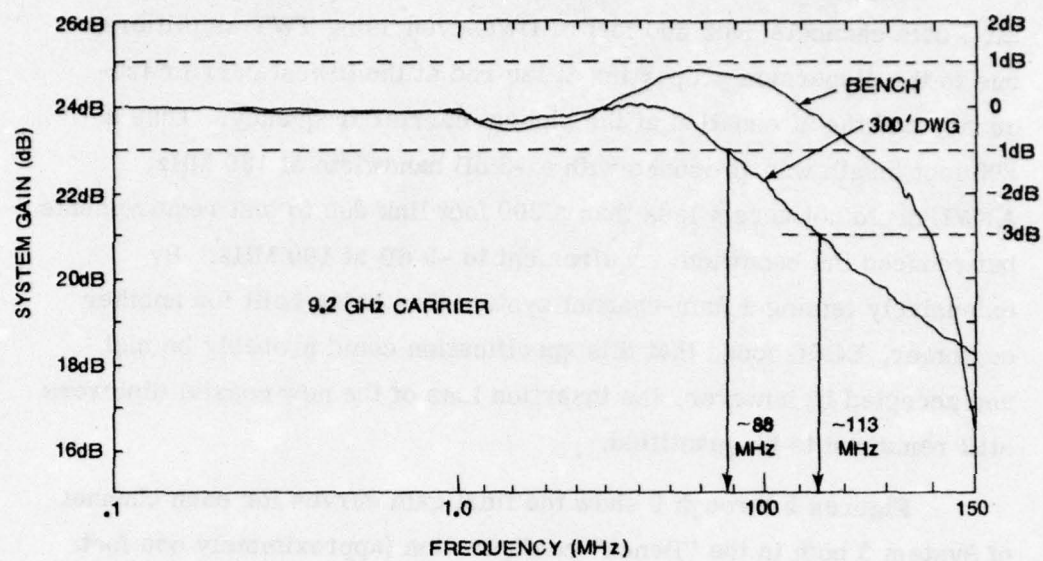


Figure 5. Channel 1 CW Data

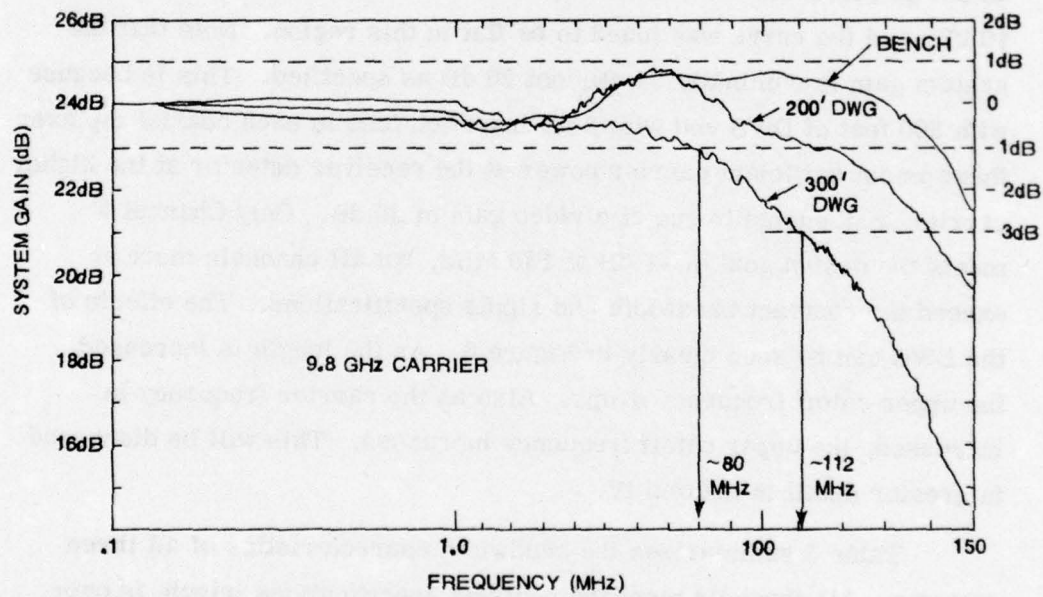
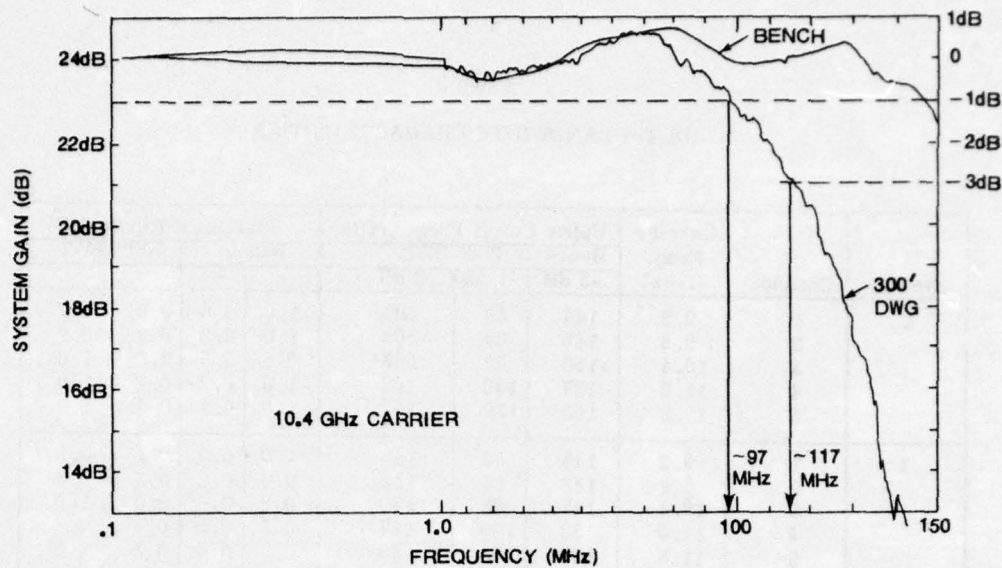


Figure 6. Channel 2 CW Data



Channel 7. Channel 3 CW Data

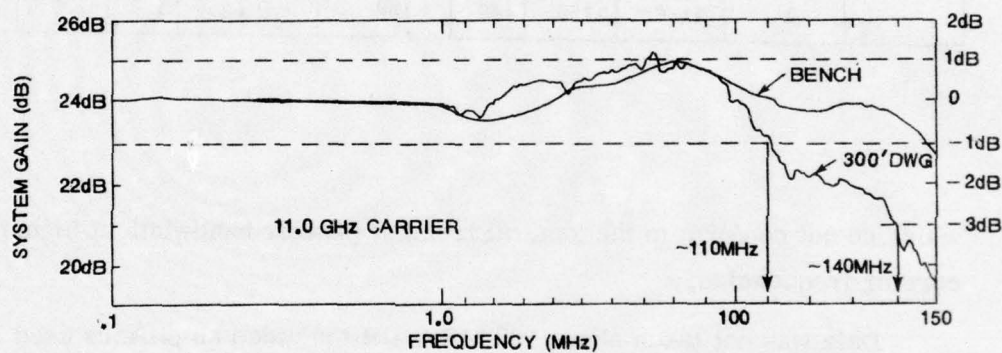


Figure 8. Channel 4 CW Data

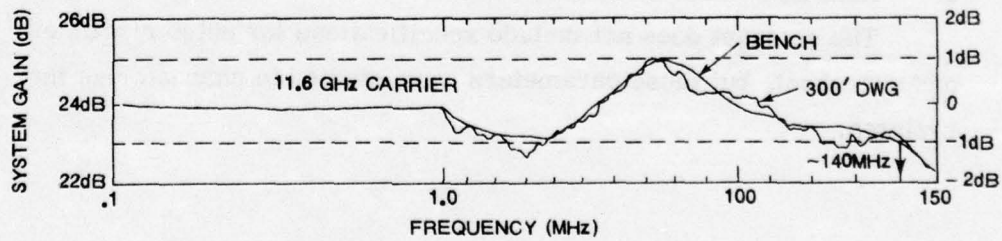


Figure 9. Channel 5 CW Data

Table 2
DLT-7 BANDWIDTH CHARACTERISTICS

System	Channel	Carrier Freq. (GHz)	Upper Cutoff Freq. (MHz)			Maximum Ripple (dB)			
			300 ¹ DWG			Bench		300 ¹ DWG	
			-3 dB	-1 dB	-3 dB	+	-	+	-
1	1	9.2	144	84	100	1.0	0.6	0.0	0.7
	2	9.8	145	84	103	1.0	0.3	0.2	0.9
	3	10.4	>150	88	133	0.6	0.5	0.0	1.0
	4	11.0	137	130	142	1.0	0.7	0.8	1.0
	5	11.6	150	130	147	1.0	0.2	0.4	1.0
2	1	9.2	145	83	145	1.0	0.3	0.1	0.9
	2	9.8	143	89	112	0.7	0.2	0.3	0.8
	3	10.4	147	88	>150	0.8	0.6	0.0	1.0
	4	11.0	133	100	117	0.5	0.5	0.6	0.6
	5	11.6	147	103	130	0.7	0.4	0.3	1.0
3	1	9.2	137	88	113	0.9	0.6	0.1	0.7
	2	9.8	>150	80	112	0.9	0.6	0.0	1.0
	3	10.4	>150	97	117	0.8	0.6	0.6	0.5
	4	11.0	>150	110	140	1.0	0.5	1.0	0.5
	5	11.6	>150	140	>150	1.0	1.0	1.0	1.0

which do not conform to the general trend of greater bandwidth at higher carrier frequencies.

Data was not taken above 150 MHz, but the video amplifiers used will limit the bandwidth to about 170 MHz on those channels with overall system bandwidths exceeding 150 MHz.

3 RISE TIME AND OVERSHOOT

The contract does not include specifications for pulse risetime and overshoot, but these parameters were studied to characterize the systems.

Various empirical studies (Reference 8) have shown a general relationship between risetime and bandwidth as follows:

$$T_r B = .35 \text{ to } .45$$

where

T_r = risetime (10 to 90 percent)

B = bandwidth (from 0 to the upper 3 dB frequency)

In the above formula the value of 0.35 matches best those circuits where the overshoot is small or zero, while 0.45 corresponds to overshoots of about 5% or greater.

Two ideal cases have been investigated theoretically, and they are in close agreement with the above. The nature of the step response of an ideal low-pass filter is a sine-integral function, yielding $T_r B = 0.51$. This response always yields an overshoot variously reported to be either 9 percent (Reference 8) or 18 percent (Reference 9). Another amplitude response of theoretical interest is the so called gaussian function. The response of a system of this kind to a step function is also a gaussian function, possessing zero overshoot and $T_r B = 0.41$.

The risetime-bandwidth product has been examined in the DLT-7 microwave systems and found to vary somewhat from the ideal and slightly from channel to channel.

Table 3 presents data from the five channels of System 3.

8. Pettit, J. M., and M. M. McWhorter, Electronic Amplifier Circuits, Theory and Design, McGraw-Hill, New York, 1961, pp 121-123.
9. Sommerfeld, A., "Partial Differential Equations in Physics," Pure and Applied Mathematics, Vol. 1, Academic Press, New York, 1949, pp 7-11.

Table 3
RISE TIME/BANDWIDTH DATA FOR SYSTEM 3 (300' DWG)

Channel	Carrier Freq. (GHz)	Bandwidth (MHz at - 3 dB)	Risetime (ns)	$T_r B$
1	9.2	113	5.1	0.58
2	9.8	112	5.1	0.56
3	10.4	117	4.7	0.55
4	11.0	140	4.0	0.56
5	11.6	150	3.8	0.57

The input was a 70 ps risetime pulse from a Tektronix 284, and the recording oscilloscope was a 1.6 ns risetime HP 183; both risetimes were much less than system risetimes so the corrections of the recorded data were small. The input pulse risetime was sufficiently shorter than the system risetime that the system approximated the ideal low pass filter responding to a step function. The observed risetime-bandwidth products were about 0.56, slightly greater than the ideal product of 0.51 for this case.

Overshoot of about 18% is observed in the pulse response with this fast risetime input (Figure 10) but disappears when the input pulse risetime is slowed to approximate that of the system (Figure 11). This has always been observed. Previous attempts to "tweak" the gain curve for a system have been unsuccessful in eliminating this overshoot with fast inputs unless the bandwidth was severely restricted.

Further experiments were run with the DLT-7 systems to attempt to characterize the relationships between risetime, bandwidth, ripple, and overshoot. A Tektronix 7704 oscilloscope and 284 pulser were used. The 3-dB bandwidth of each channel of System 2 was adjusted to 130 MHz for the bench configuration; the ripple characteristics below 130 MHz differed from channel to channel. Table 4 summarizes the observed data.

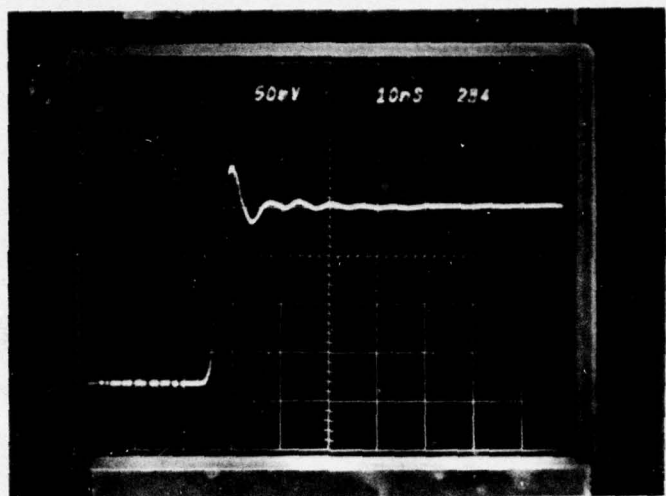


Figure 10. Response of Typical DLT-7 Channel
to 70 ps Risetime Input Pulse

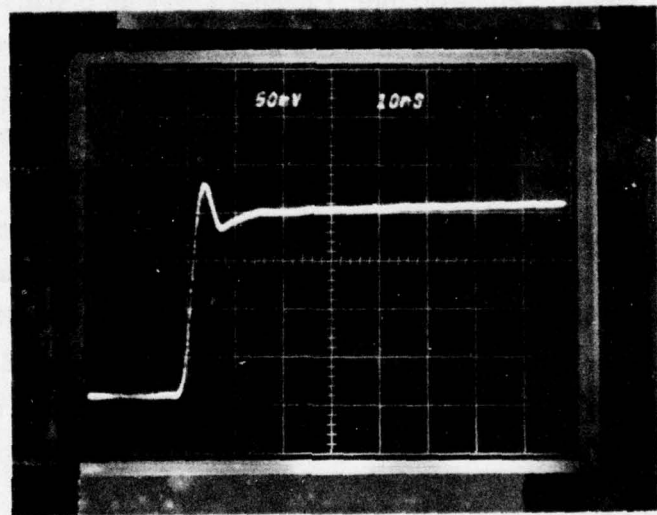


Figure 11. Response of Typical DLT-7 Channel
to Slower Risetime Input Pulse

Table 4

RISE TIME, BANDWIDTH, RIPPLE, AND OVERSHOOT
DATA FOR SYSTEM 2 (SYSTEM 3) IN BENCH CONFIGURATION

Channel	Bandwidth (MHz)	Peak Ripple 50-100 MHz (dB)	T_r (ns)	$T_r B$	Overshoot (%)
1	130	+1.0 at 50	3.7	0.48	16
2	130	-0.6 at 50	4.0	0.52	20
3	130	+0.6 at 80	3.4	0.44	18
4	130	-0.8 at 90	3.4	0.44	16
5	130	+0.8 at 50	3.7	0.48	17
5	110	+0.8 at 50	3.8	0.42	15
(System 3)					

Notice the similarity in overshoot from channel to channel despite differences in ripple. For example, Channel 3 was up 0.6 dB at 80 MHz and Channel 4 down 0.8 dB at 90 MHz yet the overshoots differed by only two percent. The $T_r B$ product is not as constant for this configuration and averages 0.47, considerably less than for System 3 with 300 feet of DWG but still close to the theoretical value of 0.51. However, due to the 10 ns/div time scale used on the oscilloscope, the risetime values in Table 4 are ± 0.5 ns. The data for Channel 5 of System 3 was taken after degrading the bandwidth to 110 MHz. It was found that the overshoot and ringing was more pronounced when the 75 ps risetime Tektronix 7704 oscilloscope was used than with the 1.6 ns risetime HP 183.

Figure 12 shows a typical fast risetime pulse response. Using the definitions of width, period, and cycles shown in Figure 12, the data of Table 4 was further examined, and the results are presented in Table 5.

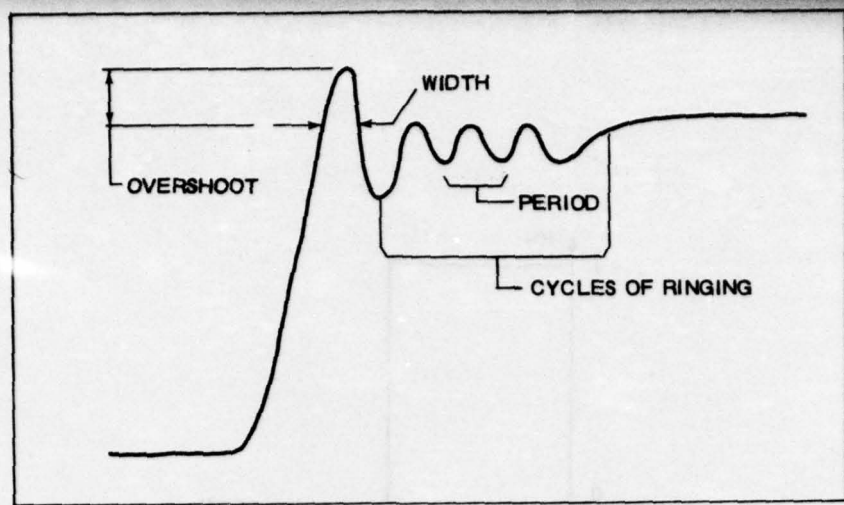


Figure 12. Characteristic Step-Function Response of DLT-7

Table 5
STEP-FUNCTION RESPONSE CHARACTERISTICS
OF SYSTEM 2 (SYSTEM 3)

Channel	Bandwidth (MHz)	Width (ns)	Cycles	Ringing Frequency (MHz)
1	130	3.5	4	161
2	130	3.5	1	161
3	130	2.0	4	154
4	130	3.2	3	133
5	130	3.0	1	159
5 (System 3)	110	4.0	2	174

The presence of the overshoot and ringing with a step input can be explained theoretically and is known as Gibb's phenomenon, (Reference 9). Consider the input function shown in Figure 13.

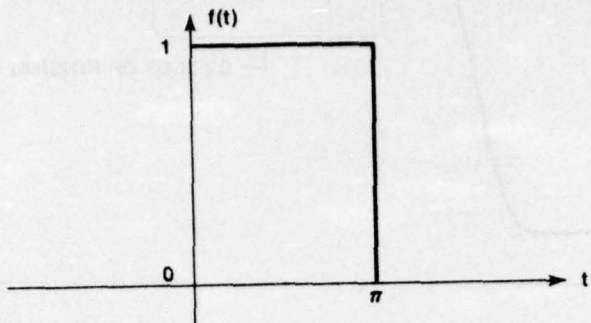


Figure 13. Input Step Function

This function is defined by

$$f(t) = \begin{cases} +1, & 0 < t < \pi \\ 0, & \pi < t < 0 \end{cases} \quad (1)$$

and is odd; i.e., its Fourier series expansion consists solely of sine terms. Suppose our system will not pass all frequencies but only those below some frequency ω_0 . The Fourier expansion using frequencies below ω_0 will only approximate $f(t)$ and involves finite integrals of the form

$$Si(x) \equiv \int_0^x \frac{\sin u}{u} du \quad (2)$$

which is known as the "sine integral" function of x and is tabulated (Reference 10). Using this notation, $f(t)$ can be approximated by

$$f(t) \approx \frac{1}{\pi} Si[\omega_0(t+1)] - \frac{1}{\pi} Si[\omega_0(t-1)] \quad (3)$$

where the x in Eq. (2) has been replaced by $\omega_0(t+1)$ and $\omega_0(t-1)$.

10. Wylie, C. R., Advanced Engineering Mathematics, McGraw-Hill, New York, 1960, p 284.

Let S_i denote the i^{th} approximation of $f(t)$ using a Fourier series expansion and the nomenclature of Reference 9. Because $f(t)$ is odd, there are no even terms so

$$S_1 = \frac{4}{\pi} \sin t \quad (4)$$

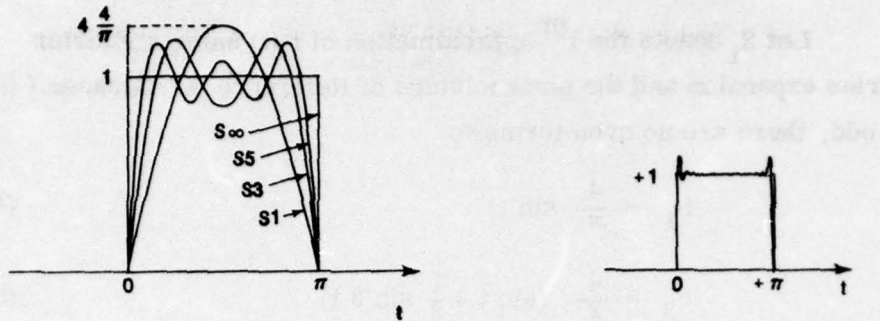
$$S_3 = \frac{4}{\pi} \left(\sin t + \frac{1}{3} \sin 3t \right) \quad (5)$$

$$S_5 = \frac{4}{\pi} \left(\sin t + \frac{1}{3} \sin 3t + \frac{1}{5} \sin 5t \right) \quad (6)$$

$$\vdots \quad \vdots \quad \vdots \quad \vdots \quad S_\infty = f(t) \quad (7)$$

S_1 has a maximum value of 1.27 at $t = \pi/2$. S_2 has a minimum at $\pi/2$ but two maxima of 1.20 at $\pi/4$ and $3\pi/4$. Similarly S_5 has maxima near $t = 0$ and $t = \pi$ (i.e., near the discontinuities). Figure 14 illustrates the successive approximations. In general the maxima and minima of S_{2n+1} lie between those of S_{2n-1} . The function $f(t)$ is approximated by successive approximations S_n which swing n times above and $n+1$ times below the line segment $f(t) = 1$. As n increases, the oscillations in the middle part of the line segment decrease; however, at the points of discontinuity $t = 0, \pi$ there is no systematic decrease in the maxima with increasing n and the approximating curves approach vertical jumps of discontinuity. The appearance of an excess above $f(t) = 1$ at the discontinuities is known as Gibb's phenomenon. Sommerfeld (Reference 9) shows that

$$\begin{aligned} S_{2n+1} &= \frac{2}{\pi} \int_0^v \frac{\sin u}{u} du \\ &= \frac{2}{\pi} \text{Si}(v) \end{aligned} \quad (8)$$



a. The approximations of the chain S_{∞} :

b. The approximation of S of very high order for the illustration of Gibb's phenomenon.

Figure 14. Illustration of Successive Fourier Approximations
(Reference 9)

and because of the properties of the sine integral function as t approaches ∞ the maxima of the S_{2n+1} approach a fixed value

$$S = \frac{2}{\pi} (1.851) \quad (9)$$

$$= 1.18$$

as n increases but remains finite.

Physically speaking, the above curves describe the output of an ideal low-pass filter, cutting off all frequencies above ω_0 , when the input pulse is an isolated rectangular fast risetime pulse (step function) (Reference 10). Thus, the appearance of overshoot on the order of 18 percent in the output of a microwave channel when driven by an input pulse of much faster risetime is to be expected.

The specifications state that the system shall operate within specifications within a range of +30°F to +120°F. For any 30°F change with a 1/2 hour soak time, the system transfer function shall vary less than ± 1 dB in amplitude which corresponds to a $\pm 10\%$ change. The test was accomplished by monitoring the amplitude of the calibration pulse with the system transmitter and receiver alternatively placed in the environment chamber. The opposite element was maintained at room temperature. The results are summarized in Tables 6 through 8.

The temperature stability of the calibration pulse generator itself was checked. The cal pulse boards for one system were placed in the environment chamber. Their outputs drove an amplifier maintained at room temperature. The results shown in Table 10 show that the calibration pulse generator is quite stable and a reliable performance monitor. The variations noted in Tables 6 to 8 are caused mostly by the video amplifiers, receiver detectors, and meter driver boards.

The temperature stability of the DWG itself was demonstrated under a previous development contract (Reference 11).

11. "Acceptance Test Report, Microwave System Development, B-1 1/5-Scale Model Project," EG&G Report AL-1005, October 1973, Contract F29601-74-C-0033, Subcontract A3HM-527162.

Table 6
TEMPERATURE TEST - SYSTEM 1

<u>Channel</u>	<u>Chassis</u>	<u>Temp (°F)</u>	Amplitude (div)		% Change	
			(pos)	(neg)	(pos)	(neg)
1	Transmitter	30	2.85	2.85	-	-
		60	2.90	2.90	1.7	1.7
		90	2.85	2.85	1.7	1.7
		120	2.90	2.90	1.7	1.7
2	Transmitter	30	2.87	2.80	-	-
		60	2.90	2.80	1.0	0.0
		90	2.85	2.80	1.7	0.0
		120	3.0	2.90	5.3	3.6
3	Transmitter	30	2.60	2.60	-	-
		60	2.70	2.62	3.7	0.7
		90	2.75	2.70	1.8	3.0
		120	2.82	2.80	2.5	3.6
4	Transmitter	30	2.70	2.75	-	-
		60	2.82	2.85	4.3	3.5
		90	2.90	2.90	4.1	1.7
		120	2.80	2.80	3.6	3.6
5	Transmitter	30	2.45	2.35	-	-
		60	2.60	2.50	5.8	6.0
		90	2.75	2.60	5.4	3.8
		120	2.82	2.65	2.5	1.9
1	Receiver	30	3.05	3.05	-	-
		60	2.90	2.90	5.2	5.2
		90	2.90	2.95	0.0	1.7
		120	2.87	2.95	1.0	0.0
2	Receiver	30	2.90	2.80	-	-
		60	2.95	2.85	1.7	1.8
		90	2.90	2.90	1.7	1.7
		120	2.80	2.80	3.6	3.6
3	Receiver	30	2.90	2.90	-	-
		60	2.90	2.90	0.0	0.0
		90	2.78	2.75	4.3	5.4
		120	2.60	2.60	6.9	5.8
4	Receiver	30	2.85	2.85	-	-
		60	2.81	2.85	1.4	0.0
		90	2.90	2.95	3.1	3.4
		120	2.90	2.95	0.0	0.0
5	Receiver	30	2.80	2.65	-	-
		60	2.80	2.65	0.0	0.0
		90	2.80	2.65	0.0	0.0
		120	2.65	2.60	5.7	1.9

Table 7
TEMPERATURE TEST - SYSTEM 2

<u>Channel</u>	<u>Chassis</u>	<u>Temp (°F)</u>	<u>Amplitude (div)</u> (pos) (neg)	<u>% Change</u> (pos) (neg)	
1	Transmitter	30	2.77 2.50	-	-
		60	2.80 2.50	1.1	0.0
		90	2.80 2.45	0.0	2.0
		120	2.77 2.40	1.1	2.0
2	Transmitter	30	2.60 2.25	-	-
		60	2.60 2.25	0.0	0.0
		90	2.50 2.25	4.0	0.0
		120	2.60 2.30	3.8	2.2
3	Transmitter	30	2.40 2.15	-	-
		60	2.50 2.20	4.0	2.3
		90	2.45 2.15	2.0	2.3
		120	2.50 2.20	2.0	2.2
4	Transmitter	30	2.60 2.25	-	-
		60	2.35 2.05	10.6	9.8
		90	2.80 2.35	16.1	12.8
		120	2.70 2.30	3.7	2.2
4	Transmitter	30	2.70 2.45	-	-
		60	2.78 2.55	2.9	3.9
		90	2.77 2.55	0.0	0.0
		120	2.85 2.60	2.8	1.9
5	Transmitter	30	2.35 2.15	-	-
		60	2.25 2.10	4.4	2.4
		90	2.40 2.20	6.2	4.6
		120	2.35 2.15	2.1	2.3
1	Receiver	30	2.70 2.40	-	-
		60	2.75 2.45	1.8	2.0
		90	2.80 2.50	1.8	2.0
		120	2.78 2.40	0.7	4.2
2	Receiver	30	2.65 2.35	-	-
		60	2.65 2.35	0.0	0.0
		90	2.62 2.35	1.2	0.0
		120	2.50 2.25	4.8	4.4
3	Receiver	30	2.35 2.10	-	-
		60	2.55 2.20	7.8	4.6
		90	2.55 2.20	0.0	0.0
		120	2.55 2.20	0.0	0.0
4	Receiver	30	2.45 2.20	-	-
		60	2.65 2.35	7.6	6.4
		90	2.75 2.35	3.6	0.0
		120	2.65 2.25	3.8	4.4
5	Receiver	30	2.40 2.25	-	-
		60	2.40 2.20	0.0	0.9
		90	2.35 2.20	2.1	0.0
		120	2.35 2.20	0.0	0.0

Table 8
TEMPERATURE TEST - SYSTEM 3

<u>Channel</u>	<u>Chassis</u>	<u>Temp (°F)</u>	Amplitude (div)		% Change	
			(pos)	(neg)	(pos)	(neg)
1	Transmitter	30	1.95	1.90	-	-
		60	1.95	1.90	0.0	0.0
		90	2.00	1.95	2.5	2.5
		120	1.95	1.90	2.5	2.5
2	Transmitter	30	1.85	1.85	-	-
		60	1.90	1.85	2.6	0.0
		90	1.95	1.80	2.6	2.8
		120	1.90	1.75	2.6	2.8
3	Transmitter	30	1.80	1.80	-	-
		60	1.80	1.80	0.0	0.0
		90	1.95	1.90	5.1	5.3
		120	1.95	1.90	0.0	0.0
4	Transmitter	30	1.95	1.70	-	-
		60	1.85	1.70	5.4	0.0
		90	1.95	1.65	5.4	3.0
		120	1.90	1.65	2.6	0.0
5	Transmitter	30	1.85	1.75	-	-
		60	1.85	1.75	0.0	0.0
		90	2.05	1.85	9.8	5.4
		120	2.20	1.90	6.8	2.6
1	Receiver	30	3.1	2.90	-	-
		60	3.1	2.95	0.0	1.7
		90	3.0	2.81	3.3	5.0
		120	2.90	2.75	3.4	2.2
2	Receiver	30	3.00	2.75	-	-
		60	2.90	2.70	3.4	1.8
		90	2.75	2.58	5.4	4.6
		120	2.60	2.50	5.8	3.2
3	Receiver	30	2.90	2.90	-	-
		60	3.00	3.00	3.3	3.3
		90	2.90	2.90	3.4	3.4
		120	2.90	2.90	0.0	0.0
4	Receiver	30	3.05	2.55	-	-
		60	3.17	2.60	3.8	1.9
		90	3.0	2.59	5.7	0.0
		120	3.05	2.60	1.6	0.0
5	Receiver	30	3.02	2.65	-	-
		60	3.1	2.70	2.6	1.8
		90	3.1	2.75	0.0	1.8
		120	3.15	2.85	1.6	3.5

4 STABILITY

The stability of the DLT-7 system was tested by several methods. First, the system amplitude and phase characteristics were monitored over a four hour period at constant temperature, and the variations recorded. It was found that amplitude and phase variation were greatest at 100 MHz.

The specifications state that the transfer function of the system shall be stable within $\pm .5$ dB in amplitude between 10 kHz and 100 MHz at a constant temperature. The results of the test are summarized in Table 9.

Channel 4 of System 2 was out of specification. A defective 2N5179 was found in the video amplifier in the transmitter. The bad transistor also showed up in the temperature tests. The channel met specification after repairs.

Table 9
STABILITY TEST RESULTS

System	Channel	Δ Amplitude at 100 MHz	
		(dB)	Δ Phase at 100 MHz
1	1	+0.2	0°
	2	+0.2	+1°
	3	+0.2	0°
	4	+0.1	-1°
	5	-0.2	-1°
2	1	-0.3	-2°
	2	-0.1	+1°
	3	-0.3	0°
	4	1.2	+5°
	5	0.0	0°
3	1	-0.5	+1°
	2	-0.2	0°
	3	-0.6	+1°
	4	-0.2	+2°
	5	0.0	+2°

Table 10
TEMPERATURE STABILITY OF CALIBRATION
PULSE GENERATORS

Temp (° F)	Channel 1 Pos-Neg (mV)		Channel 2 Pos-Neg (mV)		Channel 3 Pos-Neg (mV)		Channel 4 Pos-Neg (mV)		Channel 5 Pos-Neg (mV)	
120°	251	249	251	247	251	248	253	249	251	250
100°	251	248	251	249	251	248	251	249	250	240
80°	250	250	250	250	250	250	250	250	250	250
40°	252	248	250	251	253	252	248	252	249	251
32°	252	248	250	249	253	255	248	252	249	250

The shock and vibration tests were performed at Ball Brothers, Boulder, Colorado to demonstrate system stability under these conditions. The calibration pulse amplitudes and relative power indicators were monitored during the tests. The calibration pulses did not vary in shape or amplitude during any of the tests.

In summary, the systems were shown to be very stable even when exposed to environment changes much greater than will be encountered in normal operation.

5 DYNAMIC RANGE AND DISTORTION

Dynamic range is defined in the SOW by the following formula:

$$DR = 20 \log \left(\frac{\text{max input signal}}{\text{peak-to-peak system noise}} \right) \quad (10)$$

In this definition the maximum input signal is defined as that peak amplitude of a pure input sine wave which results in an output signal with the largest spurious harmonic down 46 dB. Thus, this definition defines harmonic distortion also. Total harmonic distortion can be

defined by taking the RMS sum of the harmonics (Reference 12) or

$$HD (\%) \equiv \left[(\% \text{ 2nd})^2 + (\% \text{ 3rd})^2 + (\% \text{ 4th})^2 + \dots \right]^{1/2} \quad (11)$$

Dynamic range is defined classically by

$$DR \equiv 20 \log \left(\frac{1 \text{ dB compression point}}{\text{tangential sensitivity}} \right) \quad (12)$$

where the tangential sensitivity is that signal level for which

$$\frac{\text{peak signal level}}{\text{peak-to-peak noise}} = 1 \quad (13)$$

and where the 1 dB compression point is that signal level which causes the output to deviate from the ideal by 10% due to overdriving (Reference 13). Using the definition of Eq. (12), all 15 channels have a dynamic range of 46 dB or greater; however, not all have all harmonics down 46 dB with the input level such that the recorded signal is up 46 dB from the peak-to-peak noise. Table 11 summarizes the harmonic distortion test results. The harmonics above the third were down sufficiently to be insignificant, and the total distortion was calculated using Eq. (11). Five of the 15 channels meet the dynamic range specification as defined in the contract. Eleven have all harmonics down by at least 40 dB with 46 dB of dynamic range. The worst channel has a total harmonic distortion of 2.36% and the best 0.30%.

12. Engelson, M., and Telewski, F., Spectrum Analyzer Theory and Applications, ARTECH House, 1974, pp 208-211.
13. The Handbook of Microwave Measurements, Vol. III, Polytechnic Press, Brooklyn.

Table 11
DYNAMIC RANGE AND HARMONIC DISTORTION

System	Channel	Harmonic Distortion		
		2nd (dB)	3rd (dB)	Total (%)
1	1	-60	-51	0.30
	2	-47	-46	0.67
	3	-46	-46	0.71
	4	-46	-42	0.93
	5	-40	-43	1.23
2	1	-42	40	1.27
	2	-44	40	1.18
	3	-45	41	1.05
	4	-34	-38	2.36
	5	-58	-38	1.27
3	1	-55	-56	1.29
	2	-43	-41	1.14
	3	-42	-39	1.37
	4	-50	-46	0.59
	5	-34	-46	2.06

To evaluate the significance of the harmonic distortion, linearity measurements were made using the LCG-2 linearity check generator.

The LCG-2 generates an extremely linear ramp output. The linear ramp is 1 μ sec in duration and bipolar at \pm 1-volt. The repetition rate of the ramp is set at 10 kilohertz. The linearity of the ramp at 500 nsec duration and at \pm 1/2-volt deviates less than 5 percent from the desired straight line.

The ramp signal is connected to the video input of the transmitter and attenuated using the input attenuators. The receiver output is connected to the oscilloscope (200 mV/div and 50 ns/div). A straight line is drawn on the output data photograph tangential at the midpoint of the curve.

Figures 15 and 16 show the output ramp recorded for Channel 1, System 1 and Channel 4, System 2, respectively. The input ramp (after attenuation) is shown in Figure 17. Straight lines have been superimposed. The effect of the greater harmonic distortion is almost indiscernable. For both channels the 1 dB compression point (10% deviation) occurs at about ± 25 mV input signal level.

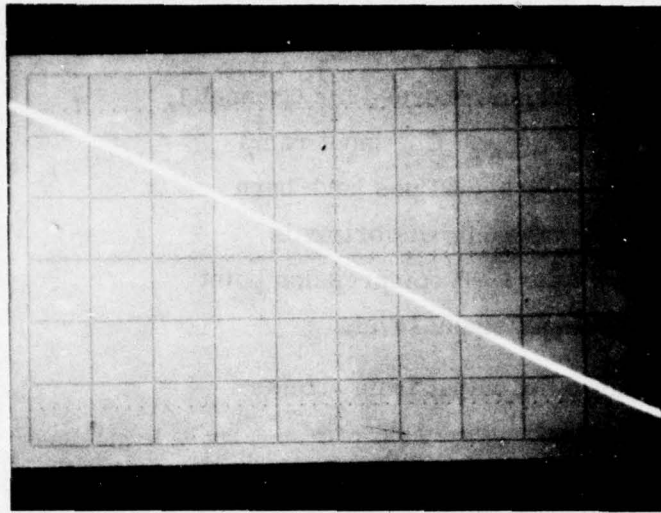
For comparison, Figure 18 shows the output from another system with much greater harmonic content:

<u>Harmonic</u>	<u>Level (dB)</u>	<u>%</u>
2nd	-36	1.58
3rd	-29	3.55
4th	-46	0.50
5th	-64	0.06

The RMS sum or total harmonic distortion is 3.9%. Again a straight line has been superimposed. In this case the effect is slightly more pronounced, and the 1 dB compression point is slightly lower at 24 mV. Figure 19 shows the harmonic spectrum for this system with a 1 MHz input sine wave with peak amplitude of ± 25 mV.

Figure 20 illustrates how the dynamic range of 46 dB or greater using the classical definition was demonstrated. Using the LCG-2 data, an input level of 26 mV was selected as a typical 1 dB compression point. This signal is shown in the top photograph, and the recorded output from one channel in the middle photograph. The gain of 24 dB is apparent. Next the input signal level is attenuated by 46 dB and the data recorded. The lower photograph shows the result for each channel of System 2. In all cases the level slightly exceeds the tangential sensitivity as defined in Eq. (13).

In summary, the systems do not meet the harmonic distortion specification on all channels, but the effect appears insignificant.



VERTICAL
200 mV
PER DIV.

HORIZONTAL
50 ns
PER DIV.

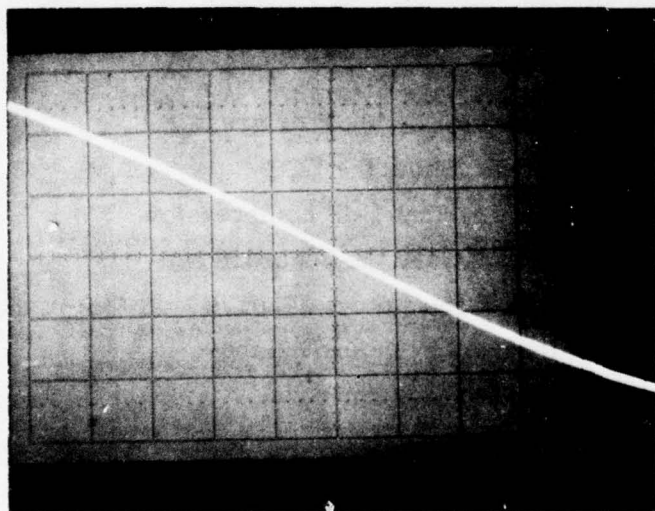
TEST: Channel 1/
System 1

DATE: 8/12/75

Comments

LCG - out

Pix #26



VERTICAL
200 mV
PER DIV.

HORIZONTAL
50 ns
PER DIV.

Comments
Channel 1/System 2

7/12/75

Pix #10

Figure 15 Channel 1 System 1 Linearity Data

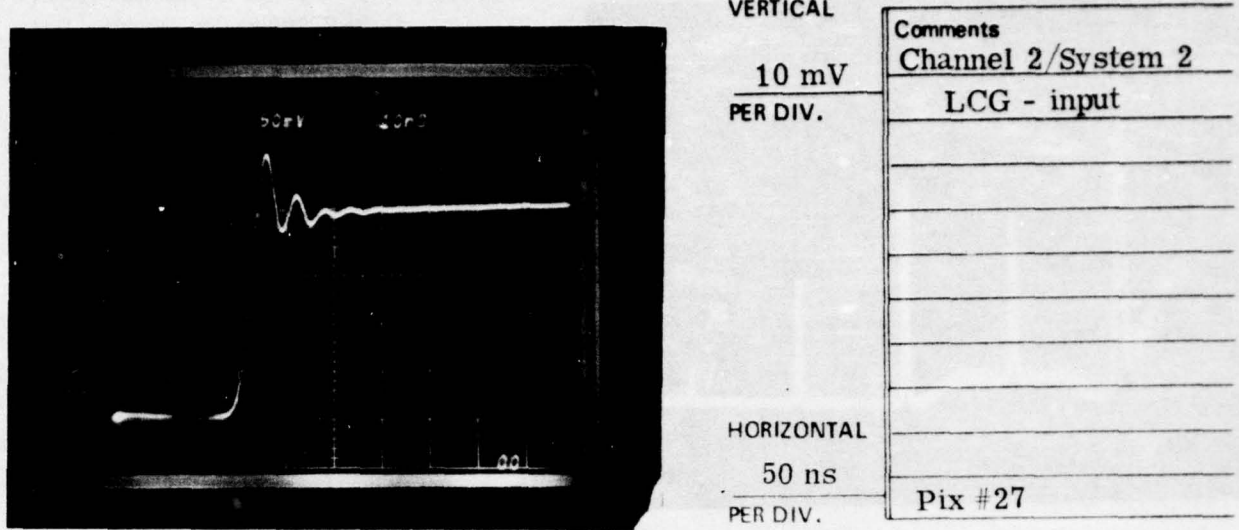


Figure 17 Transmitter Video Amplifier Input Ramp

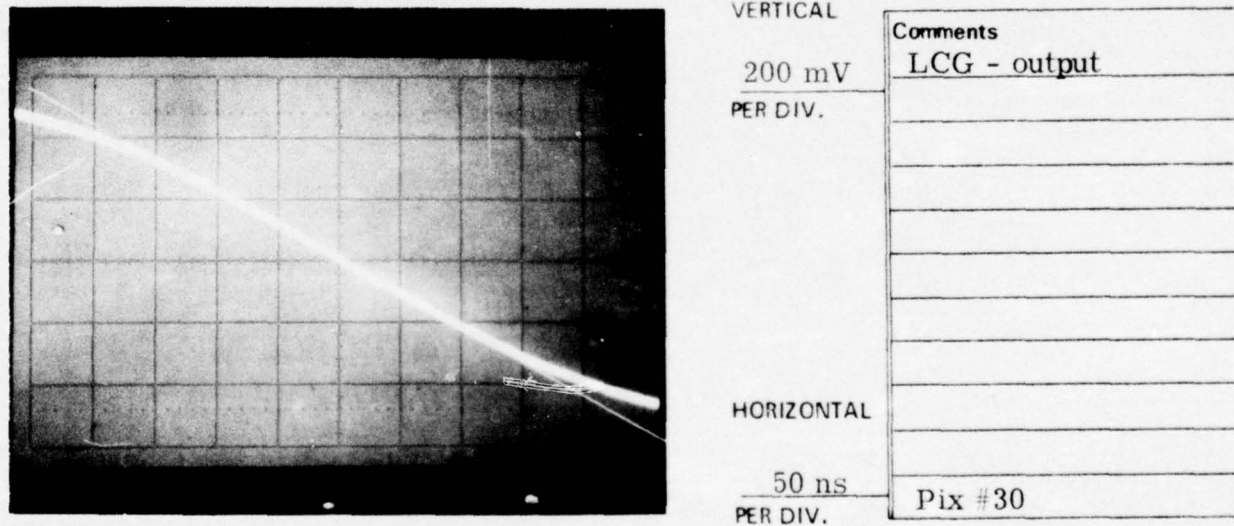
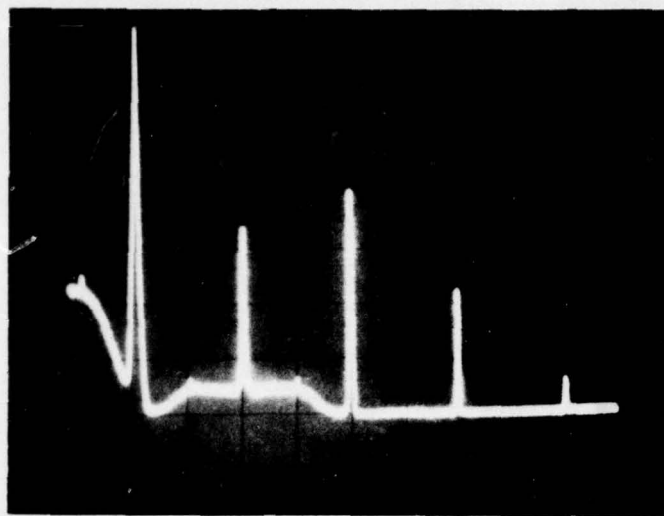


Figure 18 Ramp Output for System with 3.9 Percent Harmonic Distortion



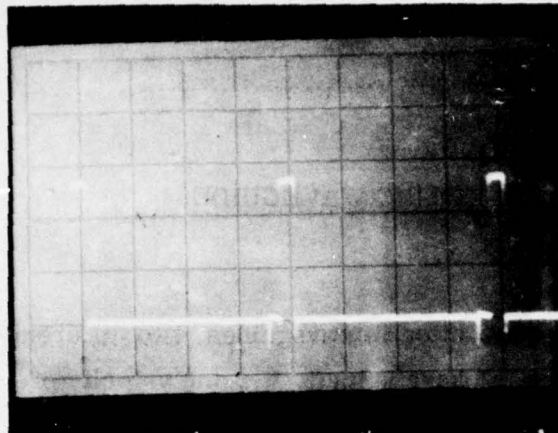
VERTICAL
10 dB
PER DIV.

Comments
Intermods of a system
with above LCG - out
input = 52 mV pp
1 MHz sine wave

HORIZONTAL
1 MHz
PER DIV.

Pix #31

Figure 19 Harmonics of System of Figure 18



VERTICAL
10mV
PER DIV.

TEST: Dynamic Range
300' Dwg.

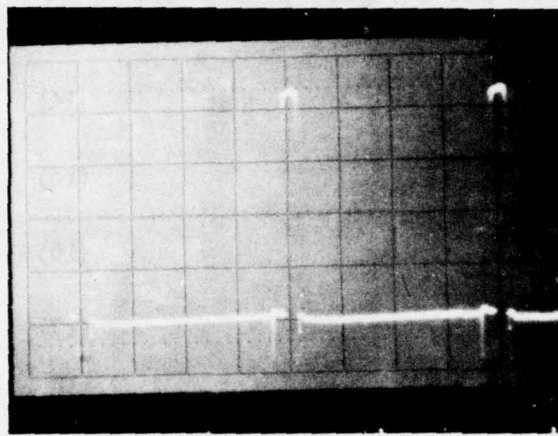
DATA: 9/12/75

Comments

System input

HORIZONTAL
5μs
PER DIV.

Pix # 32



VERTICAL
100mV
PER DIV.

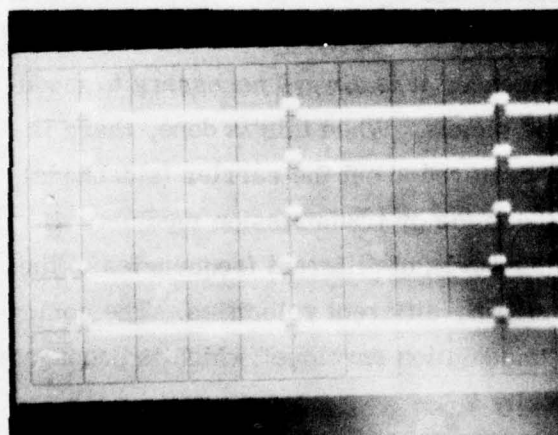
Comments

Pulse output.
of channel 1

Typical output

HORIZONTAL
5μs
PER DIV.

Pix # 33



VERTICAL
10mV
PER DIV.

Comments

Output when
input is 46dB
down.

Channel 1

Channel 2

" 3

" 4

" 5

HORIZONTAL
5μs
PER DIV.

Pix # 34

Figure 20. Dynamic Range Data

SECTION IV
EFFECTS OF THE DIELECTRIC WAVEGUIDE

1 BACKGROUND

In discussions of wave propagation in waveguides, two different velocities are encountered. One is phase velocity V_p , the velocity of propagation along the guide. The other is group velocity V_g , which in this case can be considered as the velocity of energy propagation in the direction of the axis of the guide. For waveguide propagation $V_p > V_o$ and $V_g < V_o$ where:

$$V_o = (\mu \epsilon)^{-1/2} \quad (14)$$

$$V_p = \frac{\omega}{k} \quad (15)$$

$$V_g = \frac{d\omega}{dk} \quad (16)$$

$$\omega = 2\pi f \quad (17)$$

$$k = \frac{2\pi}{\lambda} \quad (18)$$

The symbol ω denotes the angular frequency and k the wave number.

The term V_g has more significance than V_p .

In order to convey intelligence, it is always necessary to modulate a carrier frequency by some means. When this is done, there is a group of frequencies, usually centered about the carrier (sidebands), that must be propagated along the guide or transmission medium. If V_p is a function of frequency, the waves of different frequencies in the group will be transmitted with slightly different velocities. The component waves combine to form a "modulation envelope" which is propagated as a wave having the group velocity V_g .

The frequency spread of the group is assumed to be small compared with the mean frequency of the group, and the derivative is evaluated at this mean frequency.

The phenomenon of phase and group velocities can be illustrated by sketching the addition of the two sideband frequencies at a certain instant of time. Figure 21 shows two waves of slightly different frequencies combining to form a single amplitude-modulated wave. If the component waves have the same velocity, the two crests a_1 and b_1 will move along together and the maximum of the modulation envelope will move along with them at the same velocity. Under these circumstances, phase and group velocity are equal, as will be the case when the transmission path is nondispersive. Free space is an example of a nondispersive medium. Conventional waveguide and dielectric waveguide are examples of dispersive media.

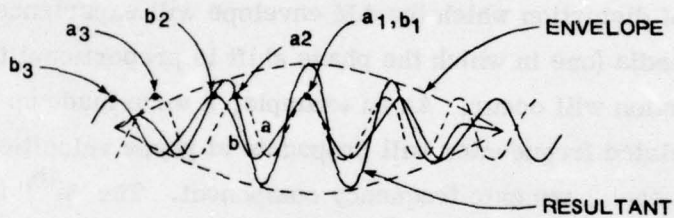


Figure 21. AM Modulation Envelope

If β is plotted as a function of ω , the phase and group velocity may be determined from the graph. Figure 22 shows such a plot for waveguide propagation. Observe that the slope $\beta/\omega = 1/V_p$ is always less than that of $dk/d\omega = 1/V_g$. So V_p is always greater than V_g , but both approach V_0 as $\omega \rightarrow \infty$.

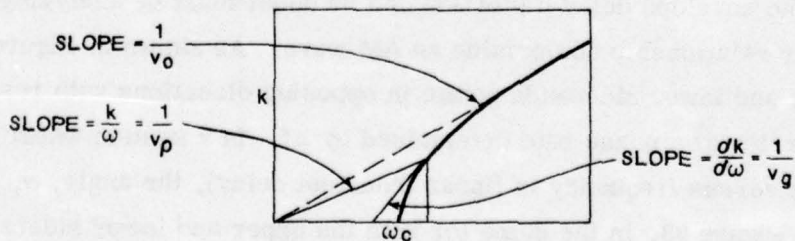


Figure 22. k vs. ω for Conventional Waveguide

The dispersion characteristics can be shown to be of the form

$$V_p = \frac{V_o}{\sqrt{1 - \left(\frac{\lambda_o}{\lambda_c}\right)^2}} \quad (19)$$

where

λ_o = free space wavelength

λ_c = cutoff frequency of waveguide

The dispersion equation indicates that the phase velocity is a nonlinear function of wavelength. The nonlinearity of the dispersion equation within the band of frequencies of an amplitude modulated signal spectrum (lower sideband to upper sideband) determines the degree of distortion which the AM envelope will experience. In a linear media (one in which the phase shift is proportional to frequency), no distortion will occur. As an example, a wave made up of harmonically related frequencies will propagate at phase velocities proportional to each harmonic frequency component. The " n^{th} " harmonic will be the same as that for the fundamental. All components, and therefore the wave itself, are delayed in time by an amount equal to the slope of the phase versus frequency characteristic.

In an amplitude modulated system, the delay to be concerned about is the envelope or group delay. The departure of the envelope delay from a constant value as a function of modulating frequency is delay distortion.

The envelope delay distortion can be understood by analyzing the vector relationship comprising an AM wave. As shown in Figure 23, the upper and lower sidebands rotate in opposing directions with respect to the carrier at a phase rate determined by Δf . In a system where the phase versus frequency is linear (constant delay), the angle, α , shown in Figure 23, is the same for both the upper and lower sidebands

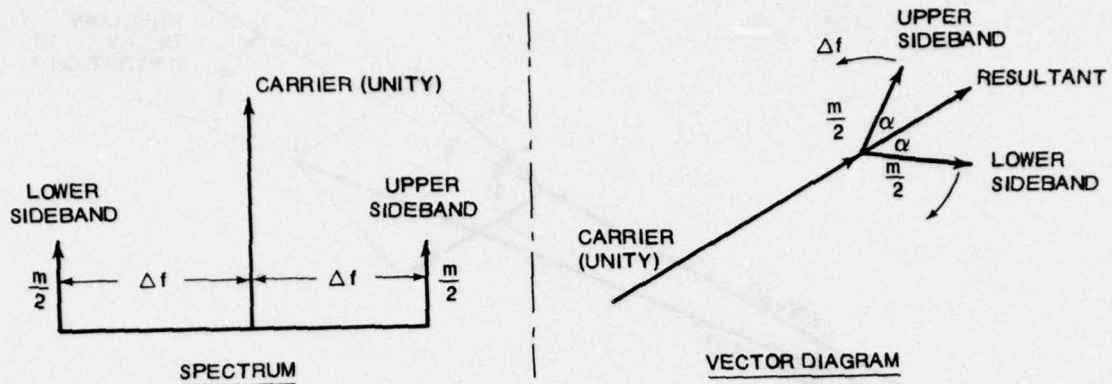


Figure 23. Spectrum and Vector Diagram of AM Modulation

with respect to the carrier or the resultant of the sidebands is always in phase with the carrier. If, however, the phase versus frequency is not linear, the symmetry of the sidebands with respect to the carrier is altered and their resultant is not in phase with the carrier as shown in Figure 24. The resultant envelope value lags the ideal linear case by an angle φ as shown in the example above. The degree of lag is a function of the frequency spacing of the sidebands with respect to the carrier and the distance over which the AM waveform propagates. The higher the modulating frequency, the more the dispersion effects become a factor. The longer the transmission path, the greater the nonsymmetry of the sidebands with respect to the carrier. From Eq. (19) for conventional hollow metal waveguides,

$$V_g = \frac{d\omega}{dk} = \frac{1}{dk/d\omega} = V_o \sqrt{1 - \left(\frac{\lambda_o}{\lambda_c}\right)^2} \quad (20)$$

where

$$\frac{dk}{d\omega} = \frac{d(1/\lambda)}{df} \quad (21)$$

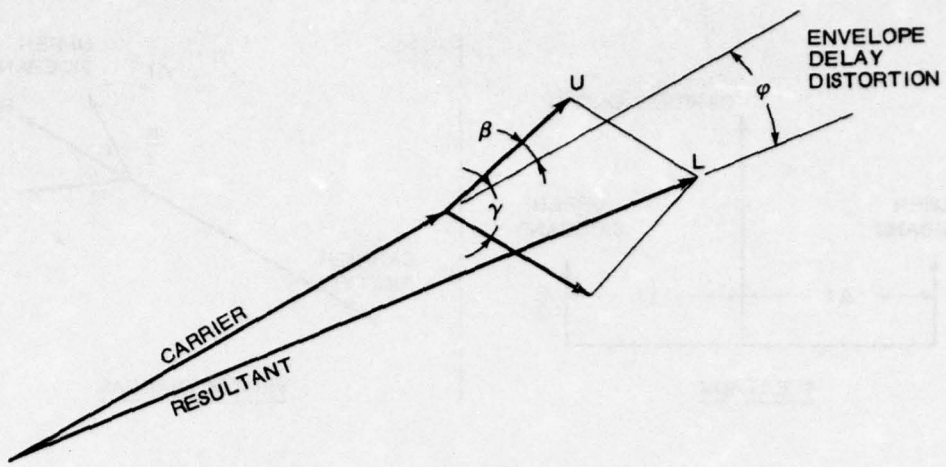


Figure 24. Envelope Delay Distortion

2 DWG ATTENUATION AND DISPERSION

We shall now consider losses in a dielectric waveguide (DWG) rod using the analysis of Elsasser (Reference 14). The radius of the rod will be A , and a cylindrical coordinate system ρ , ϕ , z , having its z axis in the axis of the rod will be used. The longitudinal components of the field vectors inside the rod are

$$\left. \begin{aligned} E_z &= AJ_n(p\rho/a) \cos n\phi e^{-i\delta z + i\omega t} \\ H_z &= BJ_n(p\rho/a) \sin n\phi e^{i\delta z + i\omega t} \end{aligned} \right\} \quad (22)$$

and outside the rod are

$$\left. \begin{aligned} E_z &= CK_n(q\rho/a) \cos n\phi e^{-i\delta z + i\omega t} \\ H_z &= DK_n(q\rho/a) \sin n\phi e^{-i\delta z + i\omega t} \end{aligned} \right\} \quad (23)$$

where p and q are dimensionless coefficients, as yet undefined, and

14. Elsasser, Walter M., "Attenuation in a Dielectric Circular Rod," Journal of Applied Physics, December 1949, pp 1193-1196

where J_n is a Bessel function; K_n is the Hankel function of the second kind. K_n decreases exponentially for large values of ρ . The other field components are obtained from Eq. (22) and Eq. (23) by differentiations. The following relations hold

$$\left. \begin{aligned} \delta^2 + p^2/a^2 &= \omega^2 \mu \epsilon_1 \\ \delta^2 - q^2/a^2 &= \omega^2 \mu \epsilon_2 \end{aligned} \right\} \quad (24)$$

where ϵ_1 and ϵ_2 refer to the inside and outside, respectively. We assume the outside to be air or vacuum and use the relative dielectric constant

$$\epsilon = \epsilon_1/\epsilon_2. \quad (25)$$

The free-space wavelength is

$$\lambda_0 = 2\pi/\omega(\mu\epsilon_2)^{1/2}, \quad (26)$$

and from Eq. (24) we obtain on eliminating δ :

$$\frac{2\pi a}{\lambda_0} = \left(\frac{p^2 + q^2}{\epsilon - 1} \right)^{1/2} \quad (27)$$

Equations (24) and (27) follow directly from Maxwell's equations; a second relation between the parameters p and q is found by fulfilling the boundary conditions on the surface of the rod. This yields the secular equation,

$$(\epsilon f + g)(f + g) - n^2 (\epsilon/p^2 + 1/q^2)(1/p^2 + 1/q^2) = 0, \quad (28)$$

where the following abbreviations have been used

$$f = \frac{J_n'(p)}{p J_n(p)}, \quad g = \frac{K_n'(q)}{q K_n(q)}, \quad (29)$$

the primes denoting differentiation. For given values of ω , n , and ϵ the Eqs (27) and (28) yield a pair of values p , q , defining a mode propagated along the rod. It is convenient to introduce two more quantities,

$$U \equiv \left[\frac{(\epsilon/p^2 + 1/q^2)}{(1/p^2 + 1/q^2)} \right]^{1/2} \quad (30)$$

$$V \equiv \left[(\epsilon f + g) / (f + g) \right]^{1/2} \quad (31)$$

By means of the last three equations, it is possible to express the entire solution in terms of p and q . First, we have from the continuity of the tangential components at the boundary

$$C/A = D/B = \left| J_n(p) \right| / \left| K_n(q) \right|, \quad (32)$$

and furthermore we find

$$B/A = D/C \approx (\epsilon_2/\mu)^{1/2} V \equiv V/\eta \quad (33)$$

where η is the intrinsic impedance of the outer space. The phase constant in the rod is given by

$$\delta/\omega = U/c \quad (34)$$

Thus $U = \lambda_0/\lambda$, the ratio of free-space wavelength to actual wavelength. The solution of Eq. (28) with the subsidiary Eq. (27) must be carried out by numerical methods. For each fixed value of n the secular equation has an infinite number of solutions, one in each interval between successive zeros of $J_n(p)$.

The dielectric loss can be calculated by a perturbation method, assuming that the power lost per wavelength along the rod is small compared to the power flowing along the rod. The mean Poynting vector, S , is clearly parallel to the rod axis, since there is no radiation perpendicular to the rod at large distances.

Then from Poynting's theorem,

$$\int S_z d\tau_2 - \int S_z d\tau_1 = -\sigma \int E^2 d\nu, \quad (35)$$

where the surfaces of integration at the left hand side are two planes perpendicular to the rod axis, and the volume at the right hand side is the section of the rod between these planes, it being assumed that $\sigma = 0$ outside the rod. Then in the limit

$$\frac{d\Phi}{dz} \equiv \frac{d}{dz} \int S_z d\tau = -\sigma \int E^2 d\tau. \quad (36)$$

Disregarding signs, we find the attenuation given by

$$\frac{1}{\Phi} \frac{d\Phi}{dz} = \frac{\sigma \int_0^a |E|^2 \rho d\rho}{\left| \int_0^a S_z \rho d\rho + \int_a^\infty S_z \rho d\rho \right|} \quad (37)$$

where

$$S_z = E_\rho H_\phi^* - E_\phi H_\rho^*. \quad (38)$$

We introduce the dimensionless quantity R by

$$\left| (1/\Phi) (d\Phi/dz) \right| \equiv \sigma \eta R. \quad (39)$$

We find then in engineering units:

$$\text{attenuation} = 2729 (\epsilon\phi/\lambda_0) R \text{ (decibels/meter)}, \quad (40)$$

where λ_0 is in cm. Here we have introduced the power factor of the material

$$\phi \equiv \sigma/\epsilon_1 \omega. \quad (41)$$

For $n = 1$, the "dipole" mode we have for R

$$R = \left| \frac{\frac{\epsilon - 1}{q} f^2 + (1/p^2) - (1/p^4)}{(1/p^2 + 1/q^2)} + (U^2 + V^2) X + \frac{4UV}{p^4}}{UX(\epsilon + V^2) + UY(1 + V^2) + \frac{2V}{p^4}(\epsilon + U^2) - \frac{2V}{q^4}(1 + U^2)} \right|,$$

where

$$\left. \begin{aligned} X &= f^2 + (2f + 1)/p^2 - 1/p^4, \\ Y &= -g^2 - (2g - 1)/q^2 + 1/q^4. \end{aligned} \right\} \quad (43)$$

The "dipole" wave, $n = 1$, may be roughly described as a sinusoidal dielectric polarization perpendicular to the rod and traveling along it. The structure of the field is fairly complicated. There is no definite cut-off so that the rod can carry waves of arbitrary length in this mode.

For sufficiently large values of $2a/\lambda_0$, the attenuation factor R tends toward the plane-wave value 0.625. For small values of $2a/\lambda_0$ the attenuation becomes small. This is attributable to the fact that the energy of the wave field is practically all outside the rod, where there is no dielectric loss. In Figure 25, R is plotted as a function of $2a/\lambda_0$, summarizing the attenuation data for all three modes for $n = 0$ and $n = 1$.

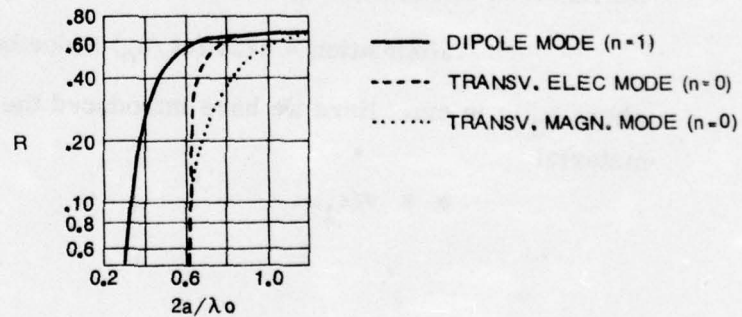


Figure 25. Attenuation Factor versus Diameter in Free-Space Wavelengths

The group velocity V_g defined in Eq. (16) can be expressed as

$$v_g = \frac{d\omega(k)}{dk} = 1 / \frac{dk(\omega)}{d\omega} \quad (44)$$

where $k = 2\pi/\lambda$ is the wave number and $\omega = 2\pi f$ is the angular frequency. This means that the wavelength is a function of the frequency in some complicated manner. We have:

$$\frac{dk}{d\omega} = \frac{d(1/\lambda)}{df}. \quad (45)$$

Using Eq. (30), we have

$$\frac{dk}{d\omega} = \frac{d(U/\lambda_0)}{df} = \frac{1}{\lambda_0} \frac{dU}{df} + U \frac{d(1/\lambda_0)}{df}. \quad (46)$$

where λ_0 is the free-space wavelength, which is related to the frequency by:

$$\lambda_0 = c/f, \quad (47)$$

c being the speed of light. Therefore, Eq. (46) becomes:

$$\frac{dk}{d\omega} = \frac{1}{\lambda_0} \frac{dU}{d(c/\lambda_0)} + U \frac{d(f/c)}{df} = \frac{2a}{\lambda_0 c} \frac{dU}{d(2a/\lambda_0)} + \frac{U}{c} \quad (48)$$

where $2a$, the diameter of the DWG, has been inserted in both the numerator and denominator of the first term. Eq. (44) now becomes:

$$\frac{v_g}{c} = \frac{1}{U + \frac{2a}{\lambda_0} \frac{dU}{d(2a/\lambda_0)}}. \quad (49)$$

Elsasser's analysis was formulated in a computer program to investigate the properties of a 5/8-inch diameter, 100-m long rod of high density polyethelene, and Table 12 gives selected results. The column headings correspond to previously defined quantities except ξ is the ratio of the field strength at $\rho = 2a$ to that at $\rho = a$; i.e., it is a measure of how quickly the field drops off in the space around the rod.

Table 12
PROPERTIES OF 5/8-INCH DIAMETER, 100-METER LONG
POLYETHYLENE ROD

<u>F(GHz)</u>	<u>p</u>	<u>q</u>	<u>2a/λ₀</u>	<u>R</u>	<u>ξ</u>	<u>U</u>	<u>Atten.</u> (db/100m)
4.09	0.8500	0.0129	0.2166	0.0014	0.4995	1.0002	0.0309
4.46	0.9250	0.0280	0.2358	0.0047	0.4981	1.0007	0.1054
4.82	1.0000	0.0517	0.2552	0.0120	0.4946	1.0021	0.2690
5.19	1.0750	0.0855	0.2748	0.0251	0.4880	1.0049	0.5620
5.58	1.1500	0.1301	0.2950	0.0455	0.4771	1.0098	1.0193
5.97	1.2250	0.1869	0.3158	0.0745	0.4612	1.0176	1.6698
6.38	1.3000	0.2573	0.3377	0.1131	0.4398	1.0290	2.5361
6.83	1.3750	0.3432	0.3612	0.1620	0.4126	1.0448	3.6312
7.31	1.4500	0.4478	0.3868	0.2209	0.3795	1.0657	4.9523
7.85	1.5250	0.5751	0.4154	0.2886	0.3409	1.0928	6.4699
8.47	1.6000	0.7313	0.4483	0.3620	0.2971	1.1267	8.1168
8.71	1.6250	0.7912	0.4606	0.3870	0.2815	1.1397	8.6768
8.95	1.6500	0.8557	0.4737	0.4118	0.2654	1.1535	9.2342
9.22	1.6750	0.9253	0.4877	0.4364	0.2490	1.1682	9.7839
9.50	1.7000	1.0005	0.5027	0.4603	0.2323	1.1838	10.3203
9.81	1.7250	1.0820	0.5189	0.4834	0.2153	1.2002	10.8378
10.14	1.7500	1.1705	0.5366	0.5054	0.1981	1.2174	11.3313
10.50	1.7750	1.2668	0.5558	0.5261	0.1808	1.2355	11.7956
10.90	1.8000	1.3719	0.5768	0.5453	0.1636	1.2543	12.2264
11.34	1.8250	1.4870	0.6000	0.5628	0.1466	1.2738	12.6201
11.82	1.8500	1.6134	0.6256	0.5786	0.1298	1.2938	12.9738
12.36	1.8750	1.7528	0.6541	0.5925	0.1135	1.3143	13.2857
14.41	1.9500	2.2691	0.7625	0.6230	0.0686	1.3774	13.9682
17.43	2.0250	2.9992	0.9223	0.6380	0.0335	1.4393	14.3047
22.17	2.1000	4.0961	1.1731	0.6415	0.0113	1.4951	14.3825
31.85	2.1750	5.9102	1.6050	0.6382	0.0020	1.5408	14.3085

Dielectric Constant = 2.560 Cutoff for Next Mode at 2a/L = 0.613

Figures 26 through 31 present this data graphically

Figure 26 shows U and v_g/c plotted for values of $2a/\lambda_0$. Also included in the phase velocity, $v_p = \lambda f$. The top axis is frequency calculated from $f 2a/c = 2a/\lambda_0$ for 5/8-inch DWG rod. The dielectric constant is taken as $\epsilon = 2.56$.

Figure 27 expands the abscissa to cover the frequency band 8.5 - 12.0 GHz for 5/8-inch rod. Plotted are v_g/c and the time t it takes a signal of a given frequency to travel 100 meters of the rod. The dispersion effects are very noticeable here. With no dispersion, v_g/c is constant with frequency and the arrival times would all be the same. Not only is there appreciable dispersion, but it is not linear.

Figure 28 expands the frequency scale even more, to 11.0 ± 0.5 GHz, and plots the arrival time and the attenuation in the rod at each frequency. From these curves, we can find the power loss and phase error after 100 meters of rod. We will look at signals transmitted on a 11.000 GHz carrier with modulation frequencies up to 500 MHz. We will look at both sidebands separately and together (single sideband (SSB; upper and lower: USB, LSB) and double sideband (DSB)). The relative time of arrival of the sidebands is obtained by subtracting the time of arrival of the carrier frequency (modulation frequency = 0) from the time of arrival of the frequency of interest. The phase error is related to this relative arrival time by

$$\varphi = 2\pi f t. \quad (50)$$

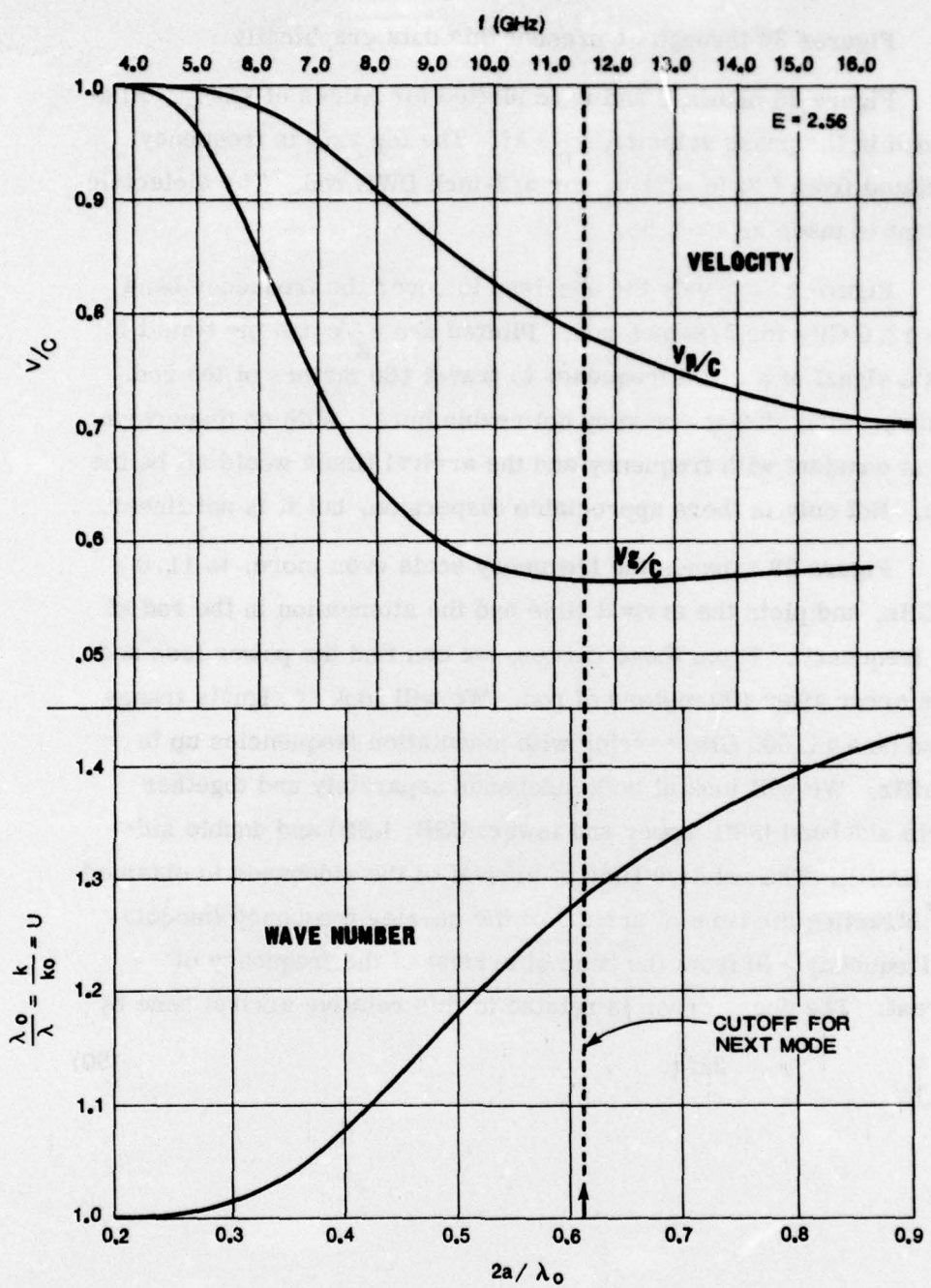


Figure 26. Velocities and Wavelength in 5/8-inch Diameter Polyethylene Rod (4.0 to 17.0 GHz)

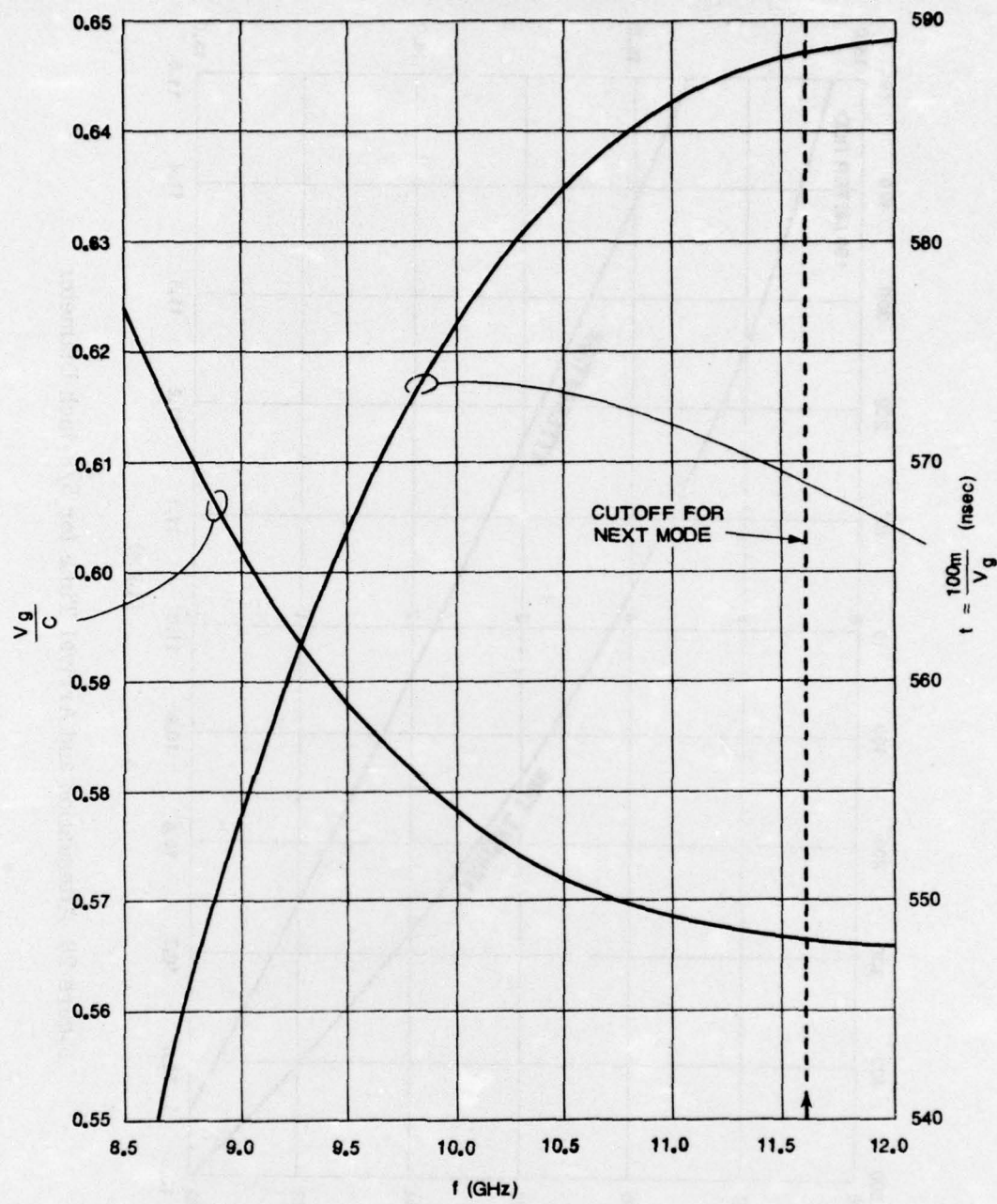


Figure 27. Group Velocity and Arrival Time for 5/8-inch Diameter Polyethylene Rod (8.5 to 12.0 GHz)

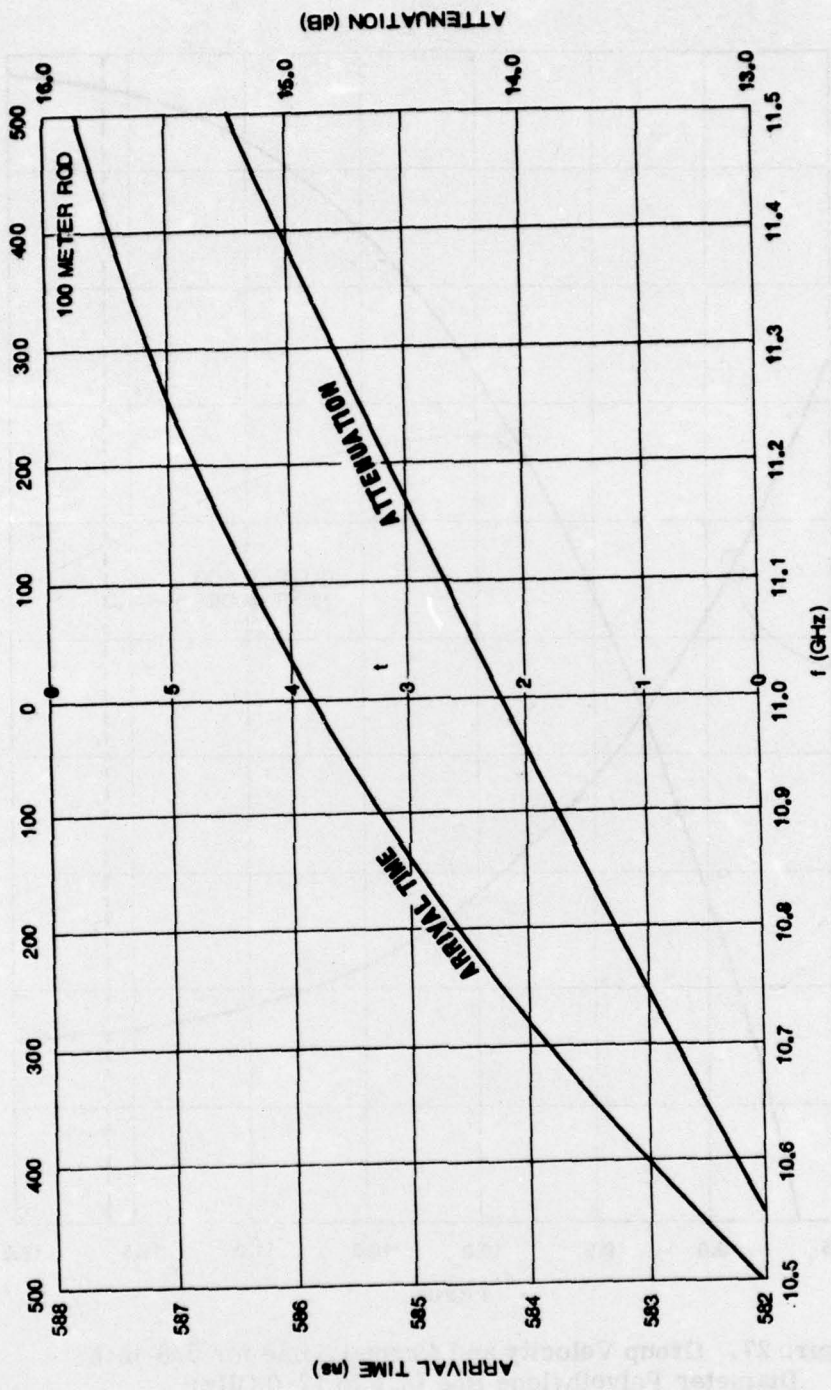


Figure 28. Attenuation and Arrival Time for 5/8-inch Diameter

We can calculate this for the DSB by adding the waves for the USB and the LSB: Let a and b be the amplitude of the LSB and the USB respectively, normalized to unity at zero modulation frequency (ZMF), as determined from the attenuation curve in Figure 27. (The 14 dB attenuation at ZMF will be discussed later.) The sum of two sine waves of arbitrary amplitude and phase is another sine wave with amplitude and phase given by:

$$p \sin(\omega t + \Theta) = A \sin(\omega t + \varphi_L) + B \sin(\omega t + \varphi_U); \quad (51)$$

$$p = \sqrt{A^2 + B^2}, \quad \Theta = \tan^{-1}(B/A) \quad (52)$$

where:

$$A = p \cos \Theta = a \cos \varphi_L + b \cos \varphi_U \quad (53)$$

$$B = p \sin \Theta = a \sin \varphi_L + b \sin \varphi_U \quad (54)$$

The power received at the end of the DWG is just:

$$P = p^2 \quad (55)$$

Figure 29 plots the relative arrival times of the sidebands with that for the DSB being obtained from Eq. (52) and the inverse of Eq. (50). Figure 30 shows the relative power (with respect to the ZMF) received for each sideband, and Figure 31 shows the phase error for each sideband.

DSB systems (such as the DLT-7) will perform poorly, both in power and phase error, for 100 meters of rod above about 150 MHz, the 3 dB point. The phase error is 7 degrees at 150 MHz; therefore dispersion effects are serious above 150 MHz.

A system using SSB modulation would have a very broad bandwidth, (well under 3 dB in power loss out to 500 MHz), but the risetime response to a step function would be very poor as the phase error becomes huge at large modulation frequency, passing 10 degrees at only 75 MHz.

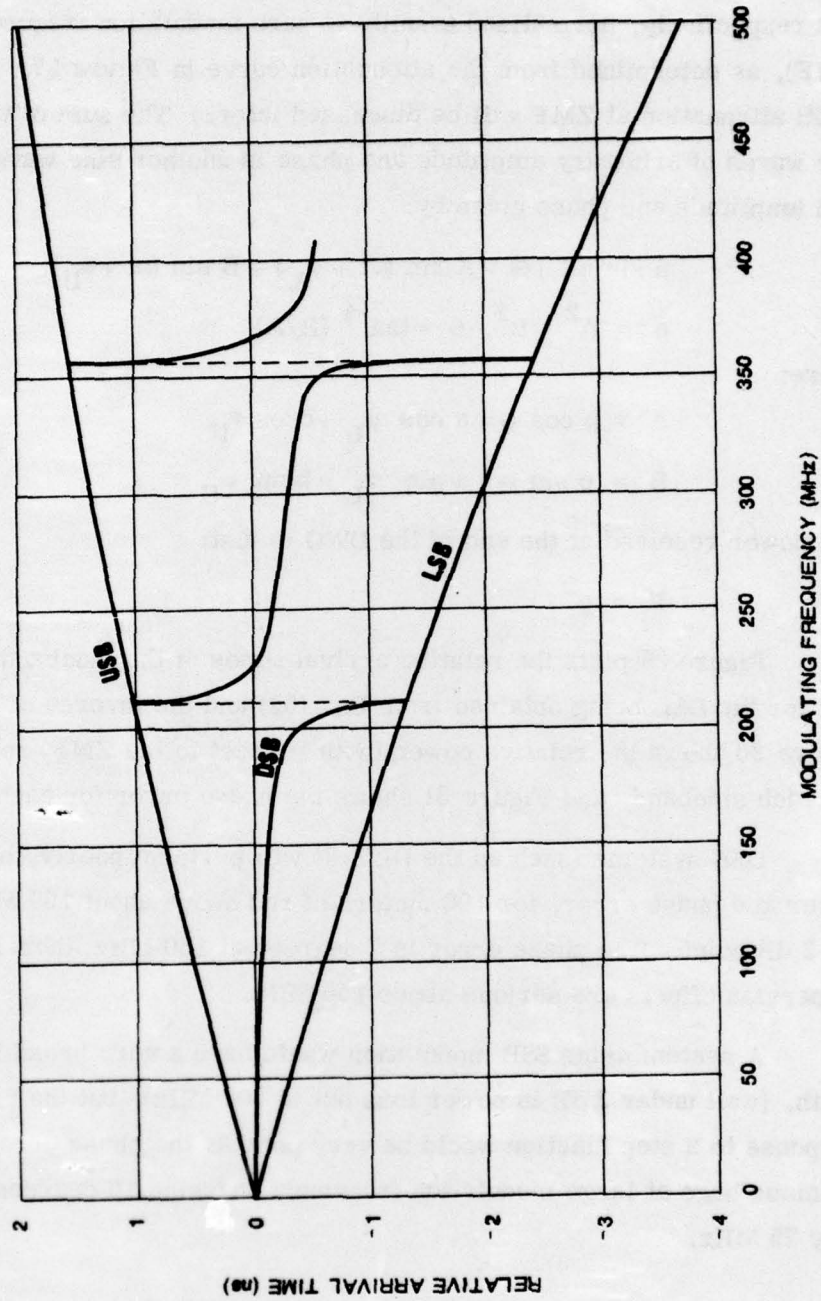


Figure 29. Relative Arrival Times for Sidebands ($f_0 = 11.0 \text{ GHz}$) for 100-Meter Long, 5/8-inch Diameter Polyethylene Rod

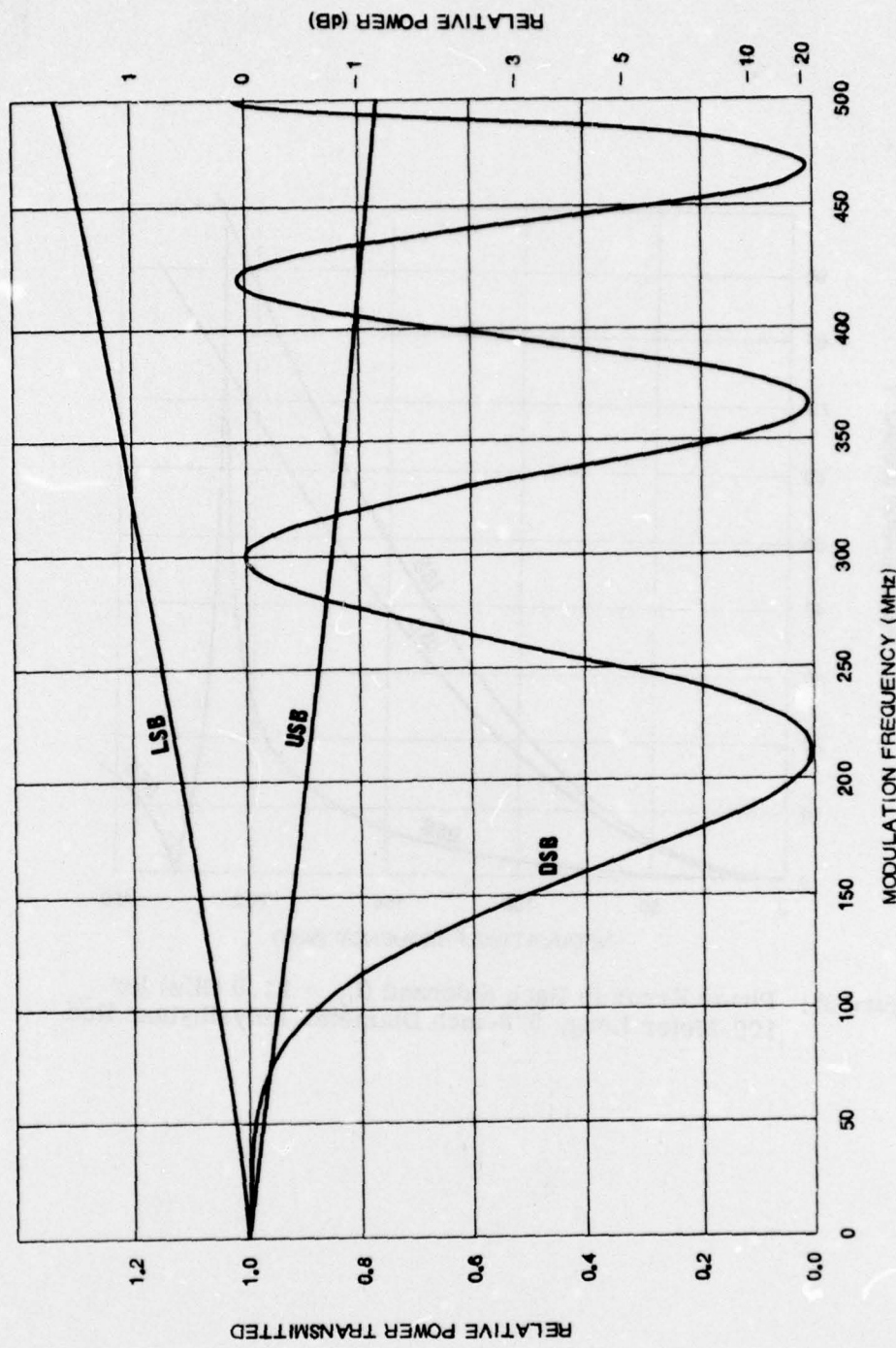


Figure 30. Relative Power Transmitted ($f_0 = 11.0$ GHz) for each Sideband for 100-Meter Long, 5/8-inch Diameter Polyethylene Rod

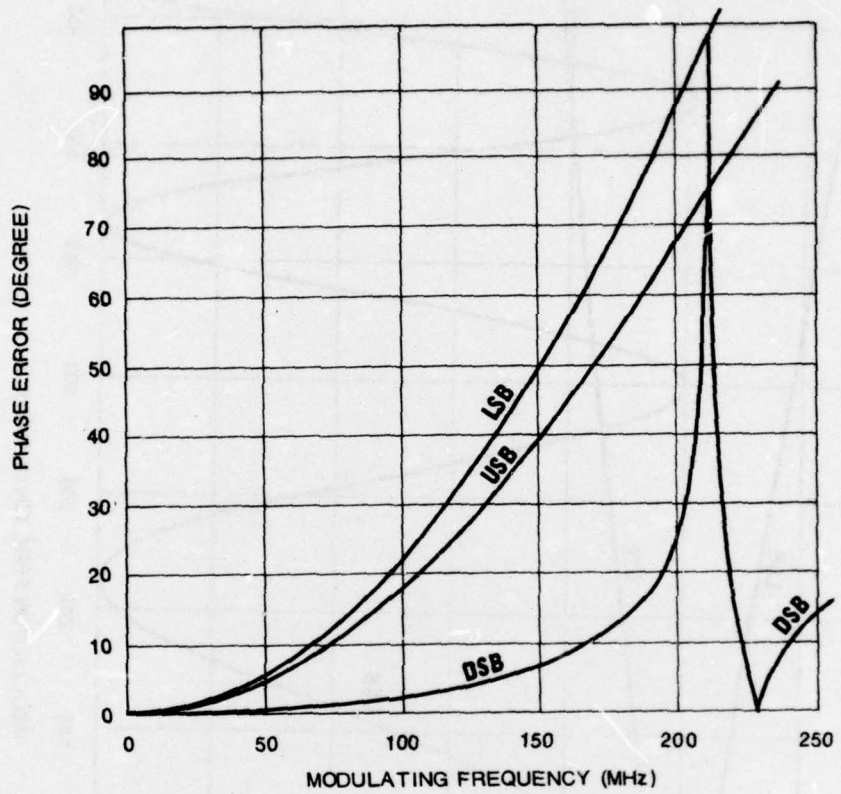


Figure 31. Phase Error in Each Sideband ($f_o = 11.0$ GHz) for 100-Meter Long, 5/8-inch Diameter Polyethylene Rod

Thus microwave systems using 5/8-inch high density polyethylene rod of 100 meters (330 feet) length have serious power loss and phase error problems, based on theoretical predictions, above about 150 MHz. Empirical data which supports these theoretical predictions will be presented in the next section.

The curves in Figures 26 through 31 are applicable to shorter DWG lengths, as the arrival times and thus the relative arrival times are proportional to the length. For 90 meters of DWG, multiply the frequency axis by 1.11.

3 EMPIRICAL DATA

A single-channel DSB DWG microwave system, similar to a channel of a DLT-7 system, was used to verify the theoretical predictions of the last section. The relative power data which corresponds to Figure 30 is shown in Figure 32. Note that 300 feet (91 meters) not 100 meters of DWG was used, but as stated earlier the difference can be removed by application of the factor 1.11 to the frequency scale.

The basic system without DWG and with $f_o = 11.0$ GHz had a 3 dB bandwidth of 340 MHz as shown by the curve labeled "Bench." With 300 feet of DWG, the 3 dB point was about 170 MHz, equivalent to about 153 MHz for 100 meters of rod. The shape of the bandpass curve is very similar to that predicted in Figure 29.

The carrier frequency f_o was changed to 9.7 GHz and the bandpass curve replotted (dotted curve in Figure 32). The 3 dB point is now found to be at about 120 MHz due to the higher dispersion at the lower frequencies. This effect was predicted by the theory and explains the problem of attaining five 130 MHz (1 dB point) data channels multiplexed over one waveguide. The choice of frequencies involves a tradeoff between dispersion at lower f_o and attenuation at higher f_o .

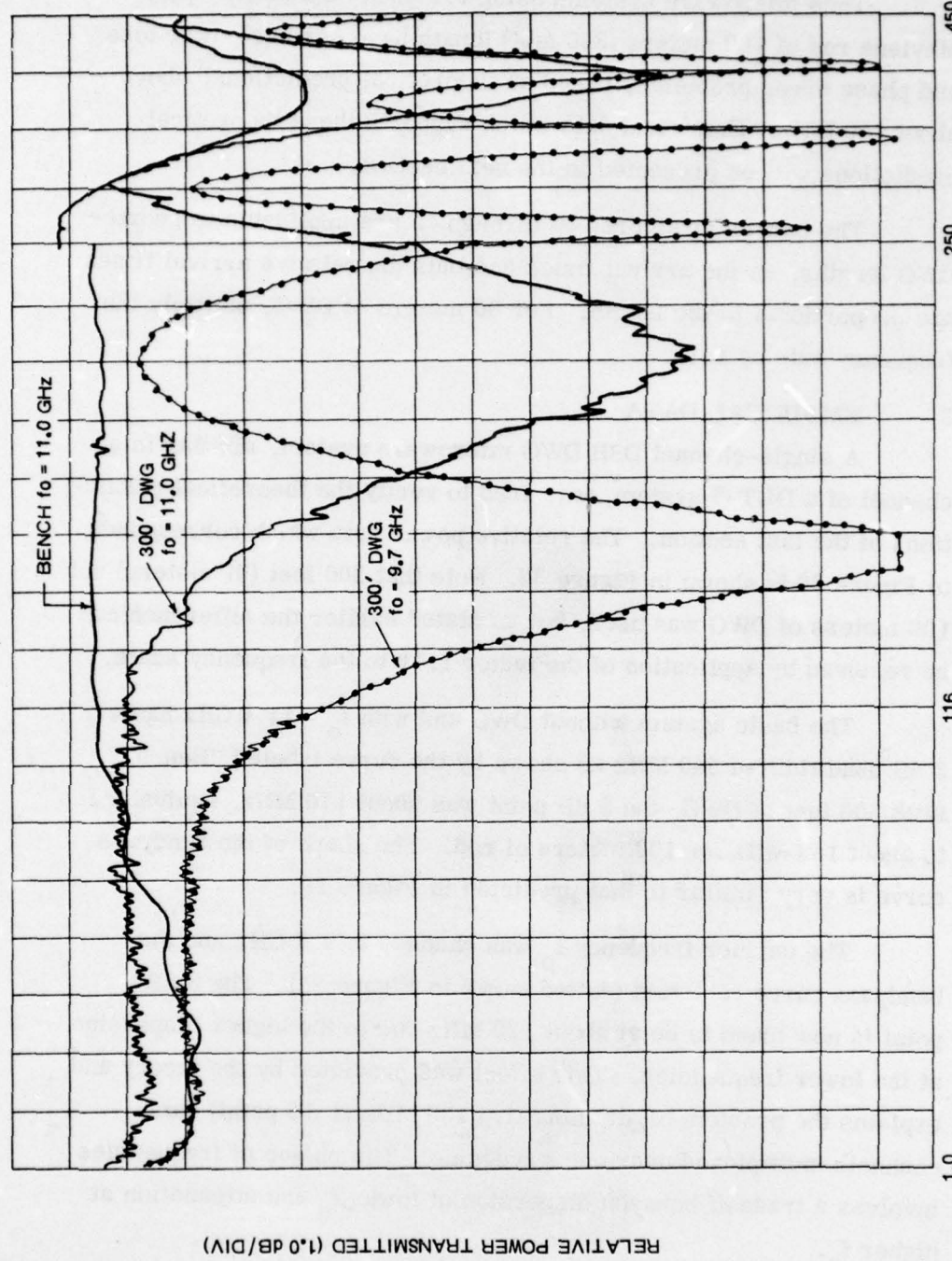


Figure 32. Empirical Relative Power Data for 5/8-inch Diameter Polyethylene Rod

Figure 33 shows attenuation versus f_o over the range 8.0 to 12.0 GHz for 300 feet of DWG. Comparing this to Figure 28, we find excellent agreement; at $f_o = 11.0$ GHz where the theory predicts 14.1 dB over 100 meters, we find about 15.5 dB over 91 meters. At 10.5 GHz the theory predicts about 12.9 dB, and we find about 14 dB.

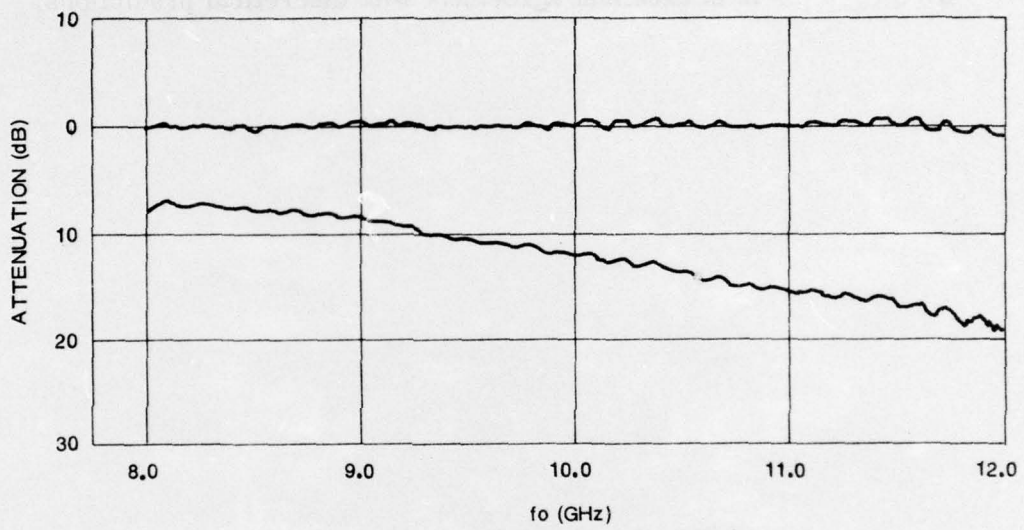


Figure 33. Empirical Attenuation Data

SECTION V
SUMMARY

EG&G has developed three five-channel multiplexed X-band microwave systems for telemetry of wideband EMP test data. The systems are much smaller in size and weight than design specifications and any previous multiplexed microwave systems built for this application. The systems meet almost all the design specifications and the deviations appear to be minor in effect. The performance of the DWG systems is in excellent agreement with theoretical predictions.

DISTRIBUTION

No. cys

1 Hq USAF, AFTAC (TAP), Patrick AFB, FL 32925
1 AFISC, (PQAL), Norton AFB, CA 92409
1 Dir Nuc Surety (SN), Stop 71
1 ASD, ENYEHM, WPAFB, OH 45433
AFWL, Stop 53
1 (HO, Dr. Minge)
2 (SUL)
5 (ELA)
1 Cdr, NSWC (730) White Oak, Silver Spring, MD 20910
1 CO, NWEF (ADS), Stop 40
2 DDC (TCA), Cameron Sta, Alexandria, VA 22314
1 Sandia Corp. (J. Reed, Div. 9354), PO Box 5800 Kirtland AFB, NM 87115
2 Lockheed M/S Co. (G. Thayn, Org. 85-70) Sunnyvale, CA 94088
1 BDM Corp. (B. Creason, ARES), 2600 Yale SE, Albuquerque, NM 87106
1 Official Record Copy (Mr. Nethers/AFWL/ELS)